On graded elements for multiphysics applications

Emílio C N Silva[1]**, Ronny C Carbonari**[1] **and Glaucio H Paulino**[2,3]

[1] Department of Mechatronics and Mechanical Systems Engineering, Escola Politécnica da Universidade de São Paulo, Av. Prof. Mello Moraes, 2231, 05508-900, São Paulo, SP, Brazil
[2] Newmark Laboratory, Department of Civil and Environmental Engineering, University of Illinois at Urbana-Champaign, 205 North Mathews Avenue, Urbana, IL 61801, USA

E-mail: ecnsilva@usp.br, ronny@usp.br and paulino@uiuc.edu

Abstract
Recently, the functionally graded material (FGM) concept has been explored in piezoelectric materials to improve properties and to increase the lifetime of bimorph piezoelectric actuators. For instance, elastic, piezoelectric, and/or dielectric properties may be graded along the thickness of a piezoceramic. Thus, the gradation of piezoceramic properties influences the performance of piezoactuators. The usual FGM modelling using traditional finite element formulation and discretization into layers gives a highly discontinuous stress distribution, which is undesirable. In this work, we focus on nonhomogeneous piezoelectric materials using a generalized isoparametric formulation based on the graded finite element concept, in which the properties change smoothly inside the element. This approach provides a continuum material distribution, which is appropriate to model FGMs. Both four-node quadrilaterals and eight-node quadrilaterals for piezoelectric FGMs were implemented using the graded finite element concept. A closed form two-dimensional analytical model of piezoelectric FGMs is also developed to check the accuracy of these finite elements and to assess the influence of material property gradation on the behavior of piezoelectric FGMs. The paper discusses and compares the behavior of piezoelectric graded elements under four loading conditions with respect to the analytical solutions (derived in this work) considering exponential variation of elastic, piezoelectric, and dielectric properties separately. The analytical solutions provide benchmark problems to verify numerical procedures (such as the finite element method and the boundary element method).

1. Introduction

Piezoelectric materials have a wide range of applications, especially in the field of sensors and actuators. Functionally graded materials (FGMs) are special materials that possess continuously graded properties and are characterized by spatially varying microstructures created by nonuniform distributions of the reinforcement phase as well as by interchanging the role of reinforcement and matrix (base) materials in a continuous manner (Suresh and Mortensen 1988, Miyamoto *et al* 1999). The smooth variation of

properties may offer advantages such as local reduction of stress concentration and increased bonding strength. Recently, this concept has been explored in piezoelectric materials to improve properties and to increase the lifetime of bimorph piezoelectric actuators (Ballato *et al* 2001, Zhu and Meng 1995). These actuators have attracted significant attention due to their simplicity and reliability. Usually, elastic, piezoelectric, and dielectric properties are graded along the thickness of an FGM piezoceramic (see figure 1). This gradation can be achieved by stacking piezoelectric composites of different compositions on top of each other (Zhu and Meng 1995, Qiu *et al* 2003, Chen *et al* 2003). Each lamina can be composed of a piezoelectric material or a composite made of

---

[3] Author to whom any correspondence should be addressed.
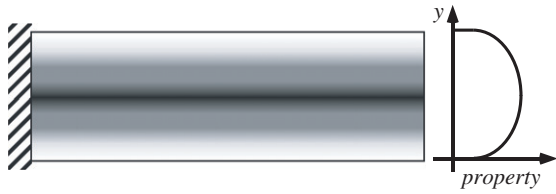
Figure 1. Smooth property variation for FGM piezoceramics.

Figure 2. Bar subjected to uniform strain (ε_0) in the x-direction and open-circuit electrical conditions ($Q = 0$). Electrodes are located at surfaces $z = 0$ and $z = h$.

piezoelectric material and a non-piezoelectric material. Many studies have been conducted on FGM piezoactuators (Zhu and Meng 1995, Zhifei 2002, Ying and Zhifei 2005, Elka *et al* 2004, Shi and Chen 2004, Almajid *et al* 2001, Taya *et al* 2003, Huang *et al* 2007, Yang and Xiang 2007).

As the applications of FGM piezoelectrics advance, new modelling techniques are also developed for such materials. The usual FGM modelling using traditional finite element (FE) formulation and discretizing the FGM into layers gives a discontinuous stress distribution (Almajid *et al* 2001, Taya *et al* 2003), which is problematic (Kim and Paulino 2002). Here we focus on the finite element method for nonhomogeneous piezoelectric materials using a generalized isoparametric formulation based on graded finite elements as developed by Santare and Lambros (2000) and Kim and Paulino (2002). In this approach, the properties change smoothly inside the element. Such an FE approach has been applied to perform different types of FGM analyses. The graded finite element concept for dynamic modeling was discussed by Banks-Sills *et al* (2002) and for wave propagation modeling by Santare *et al* (2003) and Zhang and Paulino (2007). Chakraborty and Gopalakrishnan (2003) employed the spectral finite element method based on graded finite elements to analyse the wave propagation behavior in an FGM beam subjected to either thermal or mechanical high frequency impulse loading. Finally, Thamburaj *et al* (2003) conducted studies on damage propagation in FGMs using graded finite elements.

In this work, four-node quadrilaterals (Q4) and eight-node quadrilaterals (Q8) for piezoelectric FGMs are implemented using the graded finite element concept. A two-dimensional (2D) analytical model of piezoelectric FGMs is also developed to check the accuracy of these finite elements, and to understand the influence of material property gradation in the behavior of piezoelectric FGMs. The paper discusses and compares the behavior of piezoelectric graded elements under various loading conditions with respect to the analytical solutions derived in this work. The examples consider two-dimensional models with the plane strain assumption, and four types of loading conditions. The elastic, piezoelectric, and dielectric properties are graded separately, considering exponential variations. Quantities such as displacement, electric potential, stress, strain, and electric field are investigated in the context of the examples.

This paper is organized as follows. In section 2, an analytical 2D model for FGM piezoceramics is derived based on mechanical and piezoelectric constitutive equations. Exact solutions for displacement, electric potential, stress, electric field, and electric displacement are presented. A brief description of the generalized isoparametric graded finite element formulation for FGM piezoceramics is addressed in section 3. In section 4, a comparison between numerical and analytical solutions is described. Finally, in section 5, some conclusions are inferred.
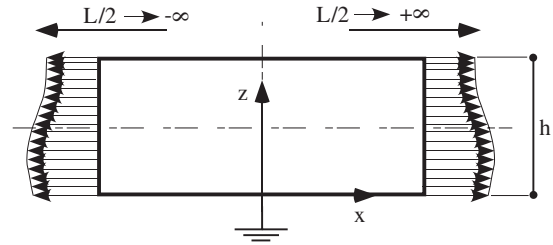
2. Some exact solutions for nonhomogeneous piezoelectricity

Exact solutions for piezoelectric FGMs are derived, which can be used as reference solutions for checking the finite element simulations based on the graded finite element concept (described ahead) and to provide insight into the influence of material property gradation on the behavior of piezoelectric materials. These solutions are an extension of those obtained by Kim and Paulino (2002) for purely elastic FGMs, and follow the same methodology and model concept.

We consider a piezoelectric FGM bar of infinite length (in the x-direction) and finite width (h) polarized in the z-direction, as shown in figure 2, under generalized plane strain conditions subjected to various load conditions. There are electrodes in the upper and lower part of the bar. The piezoelectric material is orthotropic (transversely isotropic) and it is polarized along the z-direction (see figure 2). An exponential material variation for elastic, piezoelectric, and dielectric properties are considered separately, and analytical solutions for stresses, strains, displacements, and electric potential are developed.

Starting with the linear piezoelectric constitutive equations (Ikeda 1996), we have

$$\boldsymbol{\sigma} = \mathbf{c}^E \boldsymbol{\varepsilon} - \mathbf{e}\mathbf{E}$$
$$\mathbf{D} = \mathbf{e}^t \boldsymbol{\varepsilon} + \boldsymbol{\epsilon}^S \mathbf{E} \tag{1}$$

where $\mathbf{c}^E$, $\mathbf{e}$, and $\boldsymbol{\epsilon}^S$ denote the stiffness, piezoelectric, and dielectric tensor properties of the medium, respectively. The quantities $\boldsymbol{\sigma}$, $\boldsymbol{\varepsilon}$, $\mathbf{D}$, and $\mathbf{E}$ denote the stress tensor, strain tensor, electrical displacement vector, and electric field vector, respectively. Moreover

$$\boldsymbol{\varepsilon} = \nabla_{\text{sym}}\mathbf{u}; \qquad \mathbf{E} = -\nabla\phi, \tag{2}$$

where $\mathbf{u}$ is the displacement field, ϕ is the electric potential in the piezoelectric medium, ∇ denotes the gradient operator and ∇_{sym} its symmetric part.

For a piezoelectric material from the 6mm class (Ikeda 1996) polarized in the local 3 (i.e. z) direction, the piezoelectric

constitutive equations (1) can be written in the form

$$
\begin{Bmatrix}
\sigma_{xx} \\
\sigma_{yy} \\
\sigma_{zz} \\
\sigma_{xy} \\
\sigma_{yz} \\
\sigma_{xz} \\
D_x \\
D_y \\
D_z
\end{Bmatrix}
=
\begin{bmatrix}
c_{11}^E & c_{12}^E & c_{13}^E & 0 & 0 & 0 & 0 & 0 & e_{31} \\
c_{12}^E & c_{11}^E & c_{13}^E & 0 & 0 & 0 & 0 & 0 & e_{31} \\
c_{13}^E & c_{13}^E & c_{33}^E & 0 & 0 & 0 & 0 & 0 & e_{33} \\
0 & 0 & 0 & c_{44}^E & 0 & 0 & 0 & e_{15} & 0 \\
0 & 0 & 0 & 0 & c_{44}^E & 0 & e_{15} & 0 & 0 \\
0 & 0 & 0 & 0 & 0 & c_{66}^E & 0 & 0 & 0 \\
0 & 0 & 0 & 0 & e_{15} & 0 & -\epsilon_{11}^S & 0 & 0 \\
0 & 0 & 0 & e_{15} & 0 & 0 & 0 & -\epsilon_{11}^S & 0 \\
e_{31} & e_{31} & e_{33} & 0 & 0 & 0 & 0 & 0 & -\epsilon_{33}^s
\end{bmatrix}
$$

$$
\times
\begin{Bmatrix}
\varepsilon_{xx} \\
\varepsilon_{yy} \\
\varepsilon_{zz} \\
\varepsilon_{xy} \\
\varepsilon_{yz} \\
\varepsilon_{xz} \\
-E_x \\
-E_y \\
-E_z
\end{Bmatrix} . \tag{3}
$$

Considering a plane strain assumption for the piezoelectric medium (Ikeda 1996), i.e. $\varepsilon_{xy} = \varepsilon_{yz} = \varepsilon_{yy} = 0$ and $E_y = 0$, one simplifies the piezoelectric constitutive equations as follows

$$
\begin{Bmatrix}
\sigma_{xx} \\
\sigma_{zz} \\
\sigma_{xz} \\
D_x \\
D_z
\end{Bmatrix}
=
\begin{bmatrix}
c_{11}^E & c_{13}^E & 0 & 0 & e_1 \\
c_{13}^E & c_{33}^E & 0 & 0 & e_{33} \\
0 & 0 & c_{44}^E & e_{15} & 0 \\
0 & 0 & e_{15} & -\epsilon_{11}^S & 0 \\
e_{31} & e_{33} & 0 & 0 & -\epsilon_{33}^s
\end{bmatrix}
\begin{Bmatrix}
\varepsilon_{xx} \\
\varepsilon_{zz} \\
\varepsilon_{xz} \\
-E_x \\
-E_z
\end{Bmatrix} . \tag{4}
$$

Regarding the boundary conditions of the piezoelectric bar, the lower electrode is always grounded ($\phi|_{z=0} = 0$), the x displacements are null along the edge $x = 0$, and the z displacement is null in $(x, z) = (0, 0)$. In addition, we have the following:

$$
D_x = 0; \qquad E_x = 0; \qquad \varepsilon_{xz} = 0;
$$
$$
\sigma_{zz} = 0 \Rightarrow \sigma_{xz} = 0. \tag{5}
$$

Thus, additional conditions can be obtained from the Maxwell equations, (Ikeda 1996) i.e.

$$
\frac{\partial D_x}{\partial x} + \frac{\partial D_z}{\partial z} = 0 \Rightarrow \frac{\partial D_z}{\partial z} = 0 \Rightarrow D_z = C = \text{constant}. \tag{6}
$$

From mechanical and electrical compatibility equations (Zhifei 2002), we obtain

Mechanical: $\dfrac{\partial^2 \varepsilon_{zz}}{\partial x^2} + \dfrac{\partial^2 \varepsilon_{xx}}{\partial z^2} = \dfrac{\partial^2 \varepsilon_{xz}}{\partial x \partial z} \Rightarrow \dfrac{\partial^2 \varepsilon_{xx}}{\partial z^2} = 0$

$$
\Rightarrow \varepsilon_{xx} = Az + B \tag{7}
$$

Electrical: $\dfrac{\partial E_x}{\partial z} - \dfrac{\partial E_z}{\partial x} = 0 \Rightarrow \dfrac{\partial E_z}{\partial x} = 0 \Rightarrow E_z = f(z)$, (8)

Table 1. Cases investigated.

Section 2.1	Uniform strain and open-circuit electrical conditions
Section 2.2	Uniform strain and short-circuit electrical conditions
Section 2.3	Electrical charge excitation
Section 2.4	Electrical voltage excitation

and finally, considering electrical excitation (Elka *et al* 2004), we get

$$
\int_{A_s} D_z \, dA_s = -Q \text{ (electrical charge)} \qquad \text{or}
$$
$$
\int_0^h E_z \, dz = \Delta\phi \text{ (applied voltage difference)}, \tag{9}
$$

where A_s is the surface electrode area and h is the thickness of the piezoelectric bar.

Based on the governing equations and the definition of the actual boundary value problem (involving both mechanical and electrical variables), we obtain the solution for the electric potentials and displacements in the graded piezoelectric domain (see figures 1 and 2). Exponential material variations are adopted for the following elastic, piezoelectric, and dielectric properties only:

$$
c_{11}^E = c_{11}^{0E} e^{(\beta z)}; \qquad c_{13}^E = c_{13}^{0E} e^{(\beta z)};
$$
$$
c_{33}^E = c_{33}^{0E} e^{(\beta z)}; \tag{10}
$$

$$
e_{31} = e_{31}^0 e^{(\gamma z)}; \qquad e_{33} = e_{33}^0 e^{(\gamma z)};
$$
$$
\epsilon_{33}^s = \epsilon_{33}^{0s} e^{(\alpha z)}; \tag{11}
$$

The cases investigated are summarized in table 1. The solutions are obtained by considering material variations of elastic, piezoelectric, and dielectric properties, separately, for all cases. Cases 2.1 and 2.2 consider a bar subjected to uniform strain (ε_0) in the x-direction and open-circuit electrical conditions ($Q = 0$) or short-circuit electrical conditions ($\Delta\phi = 0$), respectively. Cases 2.3 and 2.4 consider a bar subjected to electrical charge excitation per area (Q_s) or electrical voltage excitation (V_s), respectively, and no mechanical load.

The analytical results considering material gradation are presented only for case 2.1. For other cases (2.2, 2.3, and 2.4), only the results for homogeneous material (no material gradation) are presented. The corresponding Maple programs that generated these solutions are presented in appendix B. For cases 2.2, 2.3, and 2.4, due to the complex mathematical expressions, only the corresponding Maple programs are presented in appendix B. These analytical results are compared with FE simulation results in section 4 obtained using Q4 and Q8 elements.

2.1. Uniform strain and open-circuit electrical conditions

In the first case the bar is subjected to uniform strain (ε_0) in the x-direction and open-circuit electrical conditions ($Q = 0$) (see figure 2). Thus, from equations (6) and (9)

$$
Q = 0 \Rightarrow \int_{A_s} D_z \, dA_s = 0 \Rightarrow \int_{A_s} C \, dA_s = 0 \Rightarrow C = 0
$$
$$
\Rightarrow D_z = 0. \tag{12}
$$

Then, substituting (12) in equation (4), we obtain

$$\varepsilon_{xx} = \varepsilon_0 \Rightarrow \begin{Bmatrix} \sigma_{xx} \\ 0 \\ 0 \end{Bmatrix} = \begin{bmatrix} c_{11}^E & c_{13}^E & e_{31} \\ c_{13}^E & c_{33}^E & e_{33} \\ e_{31} & e_{33} & -\epsilon_{33}^s \end{bmatrix} \begin{Bmatrix} \varepsilon_0 \\ \varepsilon_{zz} \\ -E_z \end{Bmatrix}$$

$$\Rightarrow \begin{Bmatrix} -c_{11}^E \varepsilon_0 \\ -c_{13}^E \varepsilon_0 \\ -e_{31} \varepsilon_0 \end{Bmatrix} = \begin{bmatrix} -1 & c_{13}^E & e_{31} \\ 0 & c_{33}^E & e_{33} \\ 0 & e_{33} & -\epsilon_{33}^s \end{bmatrix} \begin{Bmatrix} \sigma_{xx} \\ \varepsilon_{zz} \\ -E_z \end{Bmatrix}. \quad (13)$$

The equation system (13) is solved for σ_{xx}, ε_{zz}, and E_z considering separately an exponential material variation for the elastic, piezoelectric, and dielectric properties. The quantities u_z and ϕ are also obtained from $\varepsilon_{zz} = \partial u/\partial z$ and $E_z = -\partial \phi/\partial z$, respectively.

The corresponding solution for homogeneous material (no material variation) is given by the following expressions:

$$\sigma_{xx} =$$
$$-\frac{\varepsilon_0[-c_{33}^E(e_{31})^2 - c_{33}^E c_{11}^E \epsilon_{33}^s + (c_{13}^E)^2 \epsilon_{33}^s + 2e_{31} e_{33} c_{13}^E - c_{11}^E (e_{33})^2]}{c_{33}^E \epsilon_{33}^s + (e_{33})^2}$$

$$\varepsilon_{zz} = -\frac{\varepsilon_0(e_{33} e_{31} + c_{13}^E \epsilon_{33}^s)}{c_{33}^E \epsilon_{33}^s + (e_{33})^2}$$

$$E_z = \frac{\varepsilon_0(-c_{33}^E e_{31} + c_{13}^E e_{33})}{c_{33}^E \epsilon_{33}^s + (e_{33})^2} \quad (14)$$

$$u_z = -\frac{\varepsilon_0(e_{33} e_{31} + c_{13}^E \epsilon_{33}^s)z}{c_{33}^E \epsilon_{33}^s + (e_{33})^2}$$

$$\phi = -\frac{\varepsilon_0(-c_{33}^E e_{31} + c_{13}^E e_{33})z}{c_{33}^E \epsilon_{33}^s + (e_{33})^2}.$$

The above solution recovers the solution of Kim and Paulino (2002) when there is no piezoelectric effect. Considering an exponential material variation for the *elastic property only*, one obtains the following solution:

$$\sigma_{xx} = -\frac{e^{(\beta z)} \varepsilon_0}{c_{33}^{0E} e^{(\beta z)} \epsilon_{33}^s + (e_{33})^2}$$
$$\times \left[e^{(\beta z)} (c_{13}^{0E})^2 \epsilon_{33}^s - (e_{31})^2 c_{33}^{0E} + 2e_{31} e_{33} c_{13}^{0E} \right.$$
$$\left. - c_{11}^{0E} e^{(\beta z)} c_{33}^{0E} \epsilon_{33}^s - c_{11}^{0E} (e_{33})^2 \right]$$

$$\varepsilon_{zz} = -\frac{\varepsilon_0(c_{13}^{0E} e^{(\beta z)} \epsilon_{33}^s + e_{31} e_{33})}{c_{33}^{0E} e^{(\beta z)} \epsilon_{33}^s + (e_{33})^2}$$

$$E_z = \frac{e^{(\beta z)} \varepsilon_0(-c_{33}^{0E} e_{31} + c_{13}^{0E} e_{33})}{c_{33}^{0E} e^{(\beta z)} \epsilon_{33}^s + (e_{33})^2} \quad (15)$$

$$u_z = -\frac{\varepsilon_0}{\beta e_{33} c_{33}^{0E}}$$
$$\times \left[e_{31} \beta z c_{33}^{0E} - \log(c_{33}^{0E} e^{(\beta z)} \epsilon_{33}^s + (e_{33})^2) e_{31} c_{33}^{0E} \right.$$
$$\left. + \log(c_{33}^{0E} e^{(\beta z)} \epsilon_{33}^s + (e_{33})^2) c_{13}^{0E} e_{33} \right]$$

$$\phi = -\frac{\varepsilon_0 \log\left[c_{33}^{0E} e^{(\beta z)} \epsilon_{33}^s + (e_{33})^2 \right] (-c_{33}^{0E} e_{31} + c_{13}^{0E} e_{33})}{\beta c_{33}^{0E} \epsilon_{33}^s}.$$

For an exponential material variation of the *piezoelectric property only*, the solution is:
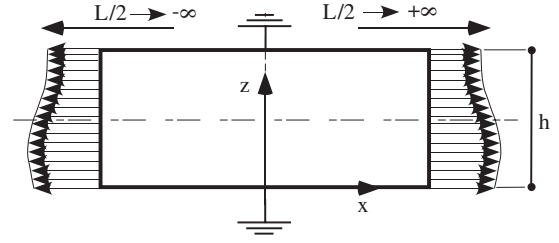
Figure 3. Bar subjected to uniform strain (ε_0) in the x-direction and short-circuit electrical conditions ($\Delta\phi = 0$).

$$\sigma_{xx} = \frac{\varepsilon_0}{(e_{33}^0)^2 e^{(2\gamma z)} + \epsilon_{33}^s c_{33}^E}$$
$$\times \left[-2e^{(2\gamma z)} e_{33}^0 c_{13}^E e_{31}^0 + e^{(2\gamma z)} (e_{31}^0)^2 c_{33}^E - (c_{13}^E)^2 \epsilon_{33}^s \right.$$
$$\left. + c_{11}^E (e_{33}^0)^2 e^{(2\gamma z)} + c_{11}^E c_{33}^E \epsilon_{33}^s \right]$$

$$\varepsilon_{zz} = -\frac{\varepsilon_0(e_{33}^0 e^{(2\gamma z)} e_{31}^0 + c_{13}^E \epsilon_{33}^s)}{(e_{33}^0)^2 e^{(2\gamma z)} + \epsilon_{33}^s c_{33}^E}$$

$$E_z = \frac{e^{(\gamma z)} \varepsilon_0(e_{33}^0 c_{13}^E - e_{31}^0 c_{33}^E)}{(e_{33}^0)^2 e^{(2\gamma z)} + \epsilon_{33}^s c_{33}^E} \quad (16)$$

$$u_z = \frac{1}{2} \frac{\varepsilon_0}{\gamma c_{33}^E e_{33}^0}$$
$$\times \left[\log((e_{33}^0)^2 e^{(2\gamma z)} + \epsilon_{33}^s c_{33}^E) c_{13}^E e_{33}^0 - \log((e_{33}^0)^2 e^{(2\gamma z)} \right.$$
$$\left. + \epsilon_{33}^s c_{33}^E) e_{31}^0 c_{33}^E - c_{13}^E 2\gamma z e_{33}^0 \right]$$

$$\phi = -\frac{\varepsilon_0 \tan^{-1}\left(e_{33}^0 e^{(\gamma z)}/\sqrt{\epsilon_{33}^s c_{33}^E} \right)(e_{33}^0 c_{13}^E - e_{31}^0 c_{33}^E)}{\gamma e_{33}^0 \left(\sqrt{\epsilon_{33}^s c_{33}^E} \right)}.$$

Finally, for an exponential material variation of the *dielectric property only*, the solution is

$$\sigma_{xx} = -\frac{\varepsilon_0}{(e_{33})^2 + \epsilon_{33}^{0s} e^{(\alpha z)} c_{33}^E}$$
$$\times \left[2c_{13}^E e_{33} e_{31} - (e_{31})^2 c_{33}^E + (c_{13}^E)^2 \epsilon_{33}^{0s} e^{(\alpha z)} \right.$$
$$\left. - c_{11}^E (e_{33})^2 - c_{11}^E c_{33}^E \epsilon_{33}^{0s} e^{(\alpha z)} \right]$$

$$\varepsilon_{zz} = -\frac{\varepsilon_0 \left[e_{33} e_{31} + c_{13}^E \epsilon_{33}^{0s} e^{(\alpha z)} \right]}{(e_{33})^2 + \epsilon_{33}^{0s} e^{(\alpha z)} c_{33}^E}$$

$$E_z = \frac{\varepsilon_0(c_{13}^E e_{33} - e_{31} c_{33}^E)}{(e_{33})^2 + \epsilon_{33}^{0s} e^{(\alpha z)} c_{33}^E}$$

$$u_z = -\frac{\varepsilon_0}{\alpha c_{33}^E e_{33}} \quad (17)$$
$$\times \left[\log((e_{33})^2 + \epsilon_{33}^{0s} e^{(\alpha z)} c_{33}^E) c_{13}^E e_{33} \right.$$
$$\left. - \log((e_{33})^2 + \epsilon_{33}^{0s} e^{(\alpha z)} c_{33}^E) e_{31} c_{33}^E + e_{31} \alpha z c_{33}^E \right]$$

$$\phi = \frac{\varepsilon_0}{\alpha (e_{33})^2}$$
$$\times \left[\log((e_{33})^2 + \epsilon_{33}^{0s} e^{(\alpha z)} c_{33}^E) c_{13}^E e_{33} - c_{13}^E \alpha z e_{33} \right.$$
$$\left. - \log((e_{33})^2 + \epsilon_{33}^{0s} e^{(\alpha z)} c_{33}^E) e_{31} c_{33}^E + e_{31} \alpha z c_{33}^E \right].$$

2.2. Uniform strain and short-circuit electrical conditions

In the second case, the bar is subjected to uniform strain (ε_0) in the x-direction and short-circuit electrical conditions ($\Delta\phi = 0$) (see figure 3).
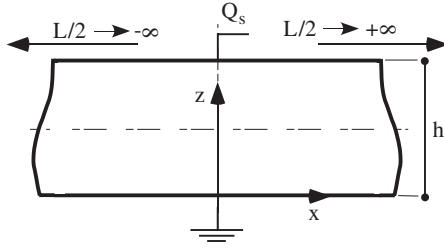
Figure 4. Bar subjected to electrical charge excitation per area (Q_s) and no mechanical load.
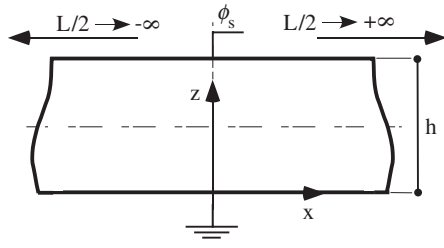
Figure 5. Bar subjected to electrical voltage excitation (V_s) and no mechanical load.

Thus, the extra boundary condition considered from equation (9) is

$$\Delta\phi = 0 \Rightarrow \int_0^h E_z \, dz = \Delta\phi = 0. \tag{18}$$

Moreover, considering equations (4) and (6), one obtains

$$\varepsilon_{xx} = \varepsilon_0; \quad D_z = C \Rightarrow \left\{ \begin{array}{c} \sigma_{xx} \\ 0 \\ C \end{array} \right\} = \left[\begin{array}{ccc} c_{11}^E & c_{13}^E & e_{31} \\ c_{13}^E & c_{33}^E & e_{33} \\ e_{31} & e_{33} & -\epsilon_{33}^s \end{array} \right]$$

$$\times \left\{ \begin{array}{c} \varepsilon_0 \\ \varepsilon_{zz} \\ -E_z \end{array} \right\} \Rightarrow \left\{ \begin{array}{c} -c_{11}^E \varepsilon_0 \\ -c_{13}^E \varepsilon_0 \\ -e_{31}\varepsilon_0 + C \end{array} \right\}$$

$$= \left[\begin{array}{ccc} -1 & c_{13}^E & e_{31} \\ 0 & c_{33}^E & e_{33} \\ 0 & e_{33} & -\epsilon_{33}^s \end{array} \right]$$

$$\times \left\{ \begin{array}{c} \sigma_{xx} \\ \varepsilon_{zz} \\ -E_z \end{array} \right\}. \tag{19}$$

The equation system (19) is solved for σ_{xx}, ε_{zz}, and E_z, and then u_z and ϕ are obtained.

The corresponding solution for homogeneous material (no material variation) is

$$\sigma_{xx} = -\frac{\left[-c_{11}^E c_{33}^E + (c_{13}^E)^2 \right] \varepsilon_0}{c_{33}^E}$$

$$\varepsilon_{zz} = -\frac{c_{13}^E \varepsilon_0}{c_{33}^E}$$

$$E_z = 0 \tag{20}$$

$$u_z = -\frac{c_{13}^E \varepsilon_0 z}{c_{33}^E}$$

$$\phi = 0.$$
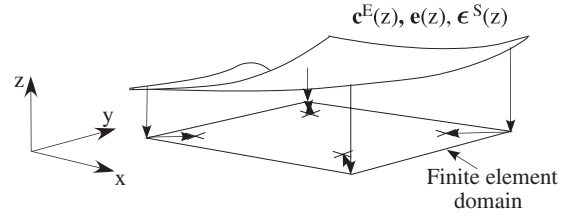
Figure 6. Continuous material distribution using a graded finite element.
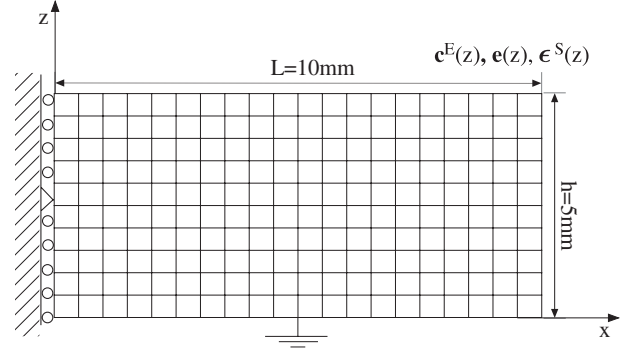
Figure 7. FE model used in the simulations (20×10 mesh). Boundary conditions and applied loads are changed according to figures 2–5.

An exponential material variation for either the elastic, piezoelectric, or dielectric properties is considered separately. For instance, considering an exponential material variation for the *elastic property*, one obtains the following solution:

$$\sigma_{xx} = -\frac{\left[\left(c_{13}^{0E}\right)^2 - c_{11}^{0E} c_{33}^{0E} \right] \varepsilon_0 e^{(\beta z)}}{c_{33}^{0E}}$$

$$\varepsilon_{zz} = -\frac{c_{13}^{0E} \varepsilon_0}{c_{33}^{0E}}$$

$$E_z = 0 \tag{21}$$

$$u_z = -\frac{c_{13}^{0E} \varepsilon_0 z}{c_{33}^{0E}}$$

$$\phi = 0.$$

Note that only the stress function is affected by material gradation. The solution considering exponential variation of the piezoelectric property is too complex to show, and only the Maple program, written to obtain it, is presented in appendix B. We notice that, in this case, the variation of the dielectric property does not influence the solution, which is identical to the homogeneous case.

2.3. Electrical charge excitation

In the third case, the bar is subjected to electrical charge excitation per area (Q_s) and no mechanical load (see figure 4). From equations (6) and (9), we obtain

$$Q = Q_s A_s \Rightarrow \int_{A_s} D_z \, dA_s = Q_s A_s \Rightarrow \int_{A_s} C \, dA_s = Q_s A_s$$

$$\Rightarrow C = Q_s \Rightarrow D_z = Q_s. \tag{22}$$
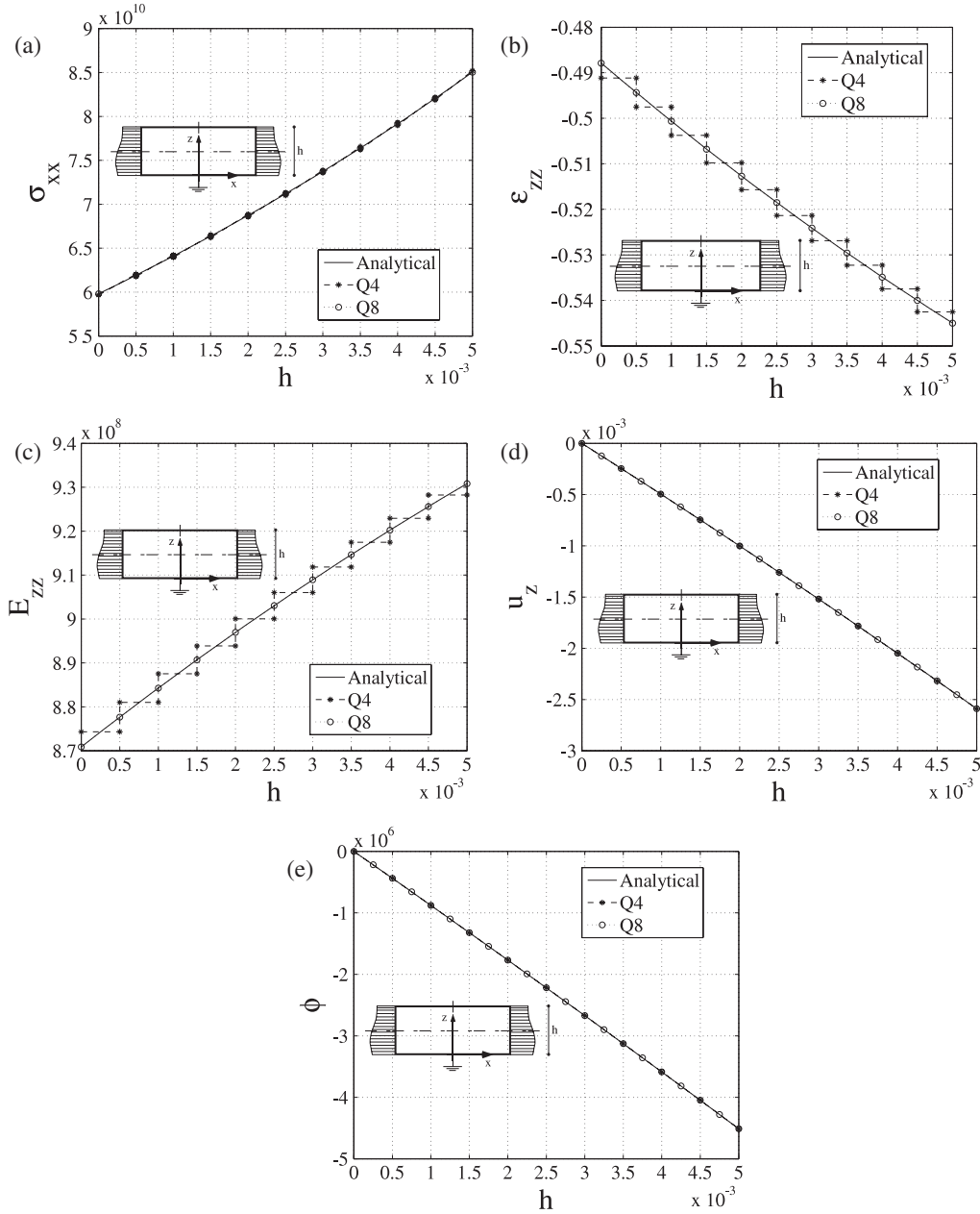
Figure 8. Comparison between numerical and analytical results for a bar *with exponential variation of elastic properties* subjected to normalized uniform strain ($\varepsilon_0 = 1$) in the *x*-direction, and open-circuit electrical conditions ($Q = 0$). All quantities are evaluated at the nodal locations: (a) stress σ_{xx}; (b) strain ε_{zz}; (c) electric field E_z; (d) displacement u_z; (e) voltage ϕ.

The boundary condition provides (Kim and Paulino 2002)

$$\int_0^h \sigma_{xx}\,\mathrm{d}z = 0; \qquad \int_0^h \sigma_{xx}z\,\mathrm{d}z = 0. \tag{23}$$

Thus, from (4) and (7), we obtain

$$\begin{Bmatrix} \sigma_{xx} \\ 0 \\ Q_s \end{Bmatrix} = \begin{bmatrix} c_{11}^E & c_{13}^E & e_{31} \\ c_{13}^E & c_{33}^E & e_{33} \\ e_{31} & e_{33} & -\epsilon_{33}^s \end{bmatrix} \begin{Bmatrix} Az + B \\ \varepsilon_{zz} \\ -E_z \end{Bmatrix}$$

$$\Rightarrow \begin{Bmatrix} -c_{11}^E (Az + B) \\ -c_{13}^E (Az + B) \\ -e_{31} (Az + B) + Q_s \end{Bmatrix} = \begin{bmatrix} -1 & c_{13}^E & e_{31} \\ 0 & c_{33}^E & e_{33} \\ 0 & e_{33} & -\epsilon_{33}^s \end{bmatrix}$$

$$\times \begin{Bmatrix} \sigma_{xx} \\ \varepsilon_{zz} \\ -E_z \end{Bmatrix}. \tag{24}$$

The equation system (24) together with equations (23) are solved for σ_{xx}, ε_{zz}, and E_z, and then, u_z and ϕ are obtained. The corresponding homogeneous solution (no material variation) obtained is

$$\sigma_{xx} = 0$$

$$\varepsilon_{zz} = \frac{(-e_{33}c_{11}^E + c_{13}^E e_{31})Q_S}{-c_{33}^E(e_{31})^2 + 2e_{31}e_{33}c_{13}^E + (c_{13}^E)^2\epsilon_{33}^S - c_{33}^E c_{11}^E \epsilon_{33}^S - c_{11}^E(e_{33})^2}$$

$$E_z = \frac{((c_{13}^E)^2 - c_{33}^E c_{11}^E)Q_S}{-c_{33}^E(e_{31})^2 + 2e_{31}e_{33}c_{13}^E + (c_{13}^E)^2\epsilon_{33}^S - c_{33}^E c_{11}^E \epsilon_{33}^S - c_{11}^E(e_{33})^2}$$

2413
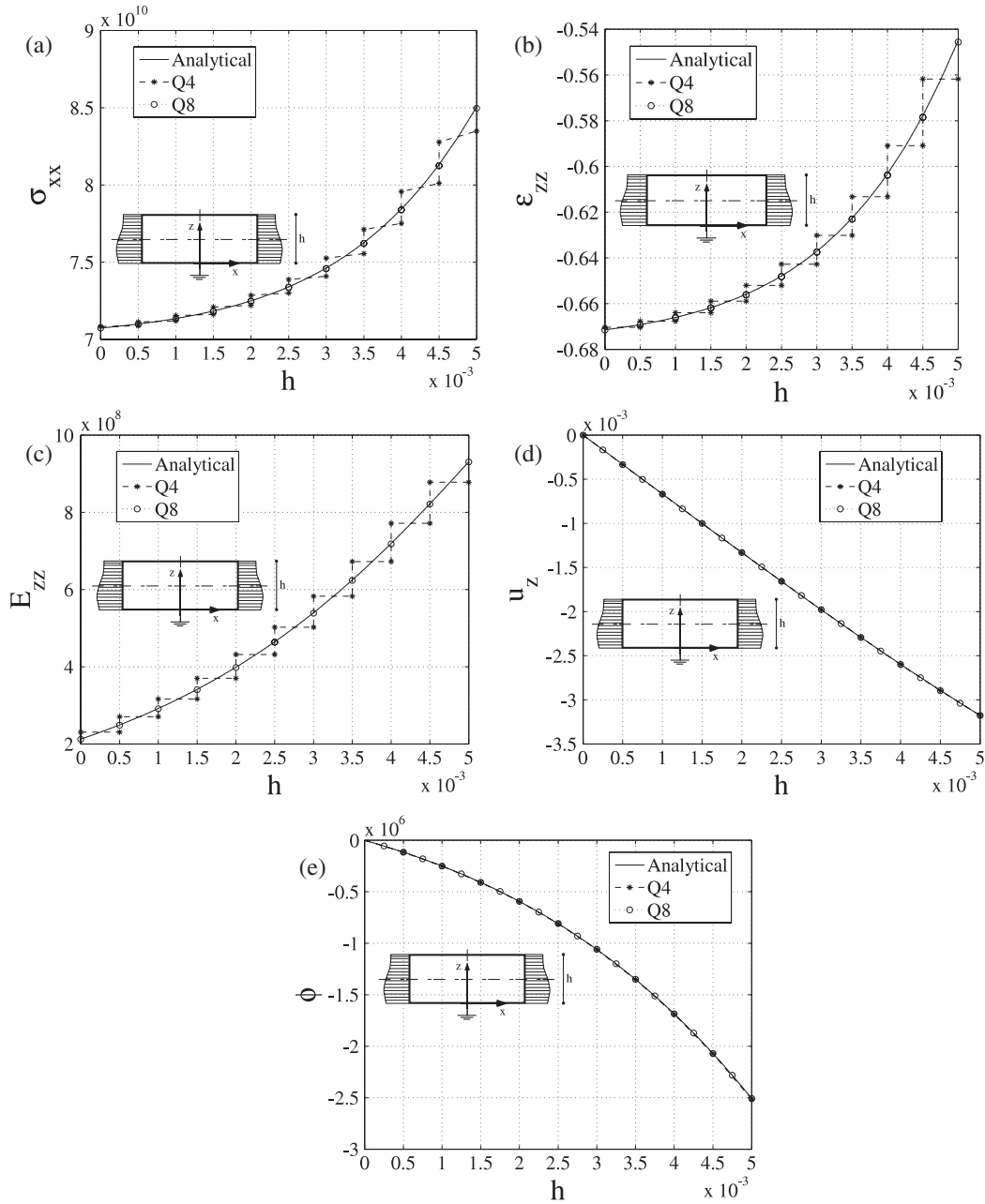
Figure 9. Comparison between numerical and analytical results for a bar *with exponential variation of piezoelectric properties* subjected to normalized uniform strain ($\varepsilon_0 = 1$) in the x-direction, and open-circuit electrical conditions ($Q = 0$). All quantities are evaluated at the nodal locations: (a) stress σ_{xx}; (b) strain ε_{zz}; (c) electric field E_z; (d) displacement u_z; (e) voltage ϕ.

$$u_z = \frac{(-e_{33}c_{11}^E + c_{13}^E e_{31})Q_S z}{-c_{33}^E(e_{31})^2 + 2e_{31}e_{33}c_{13}^E + (c_{13}^E)^2\epsilon_{33}^S - c_{33}^E c_{11}^E \epsilon_{33}^S - c_{11}^E(e_{33})^2}$$

$$\phi =$$
$$-\frac{((c_{13}^E)^2 - c_{33}^E c_{11}^E)Q_S z}{-c_{33}^E(e_{31})^2 + 2e_{31}e_{33}c_{13}^E + (c_{13}^E)^2\epsilon_{33}^S - c_{33}^E c_{11}^E \epsilon_{33}^S - c_{11}^E(e_{33})^2}.$$
$$(25)$$

The other solutions that consider exponential variation of either elastic, piezoelectric, or dielectric properties are too complex to show, and only the Maple program, written to obtain them, is presented in appendix B.

2.4. Electrical voltage excitation

In the fourth case, the bar is subjected to electrical voltage excitation (V_s) and no mechanical load (see figure 5).

From equation (9)

$$\int_0^h E_z \, \mathrm{d}z = V_s. \qquad (26)$$

The boundary condition provides (Kim and Paulino 2002)

$$\int_0^h \sigma_{xx} \, \mathrm{d}z = 0; \qquad \int_0^h \sigma_{xx} z \, \mathrm{d}z = 0, \qquad (27)$$
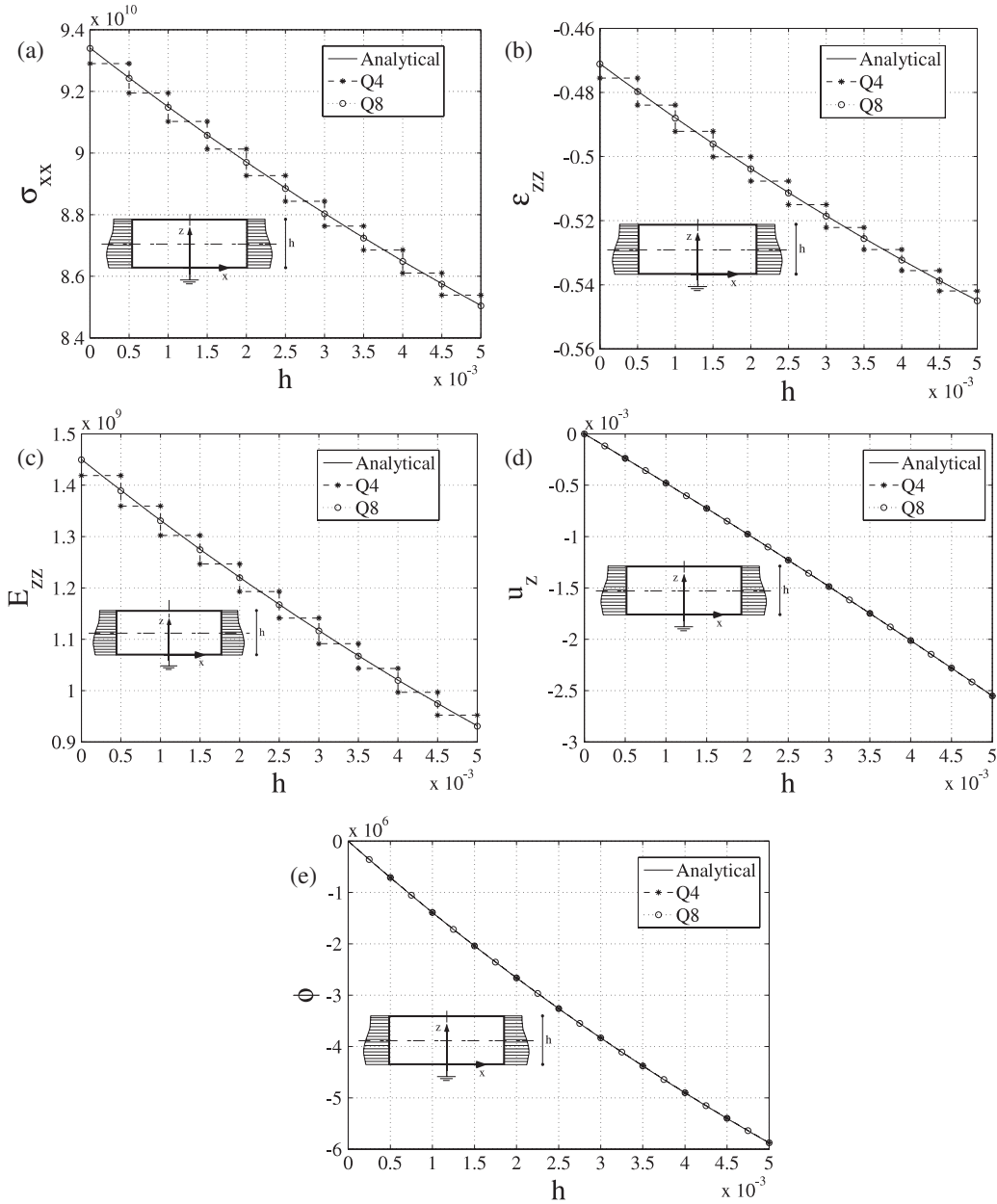
Figure 10. Comparison between numerical and analytical results for a bar *with exponential variation of dielectric properties* subjected to normalized uniform strain ($\varepsilon_0 = 1$) in the x-direction, and open-circuit electrical conditions ($Q = 0$). All quantities are evaluated at the nodal locations: (a) stress σ_{xx}; (b) strain ε_{zz}; (c) electric field E_z; (d) displacement u_z; (e) voltage ϕ.

Considering equations (4), (6), and (7), we obtain

$$D_z = C \Rightarrow \begin{Bmatrix} \sigma_{xx} \\ 0 \\ C \end{Bmatrix} = \begin{bmatrix} c_{11}^E & c_{13}^E & e_{31} \\ c_{13}^E & c_{33}^E & e_{33} \\ e_{31} & e_{33} & -\epsilon_{33}^s \end{bmatrix} \begin{Bmatrix} Az + B \\ \varepsilon_{zz} \\ -E_z \end{Bmatrix}$$

$$\Rightarrow \begin{Bmatrix} -c_{11}^E(Az + B) \\ -c_{13}^E(Az + B) \\ -e_{31}(Az + B) + C \end{Bmatrix} = \begin{bmatrix} -1 & c_{13}^E & e_{31} \\ 0 & c_{33}^E & e_{33} \\ 0 & e_{33} & -\epsilon_{33}^s \end{bmatrix}$$

$$\times \begin{Bmatrix} \sigma_{xx} \\ \varepsilon_{zz} \\ -E_z \end{Bmatrix}. \tag{28}$$

The equation system (28) together with equations (27) are solved for σ_{xx}, ε_{zz}, and E_z, and then, u_z and ϕ are obtained. The corresponding *homogeneous solution* (no

material variation) obtained is

$$\sigma_{xx} = 0$$

$$\varepsilon_{zz} = \frac{(-e_{33}c_{11}^E + c_{13}^E e_{31})V_S}{(-c_{11}^E c_{33}^E + (c_{13}^E)^2)h}$$

$$E_z = -\frac{V_S}{h}$$

$$u_z = \frac{(-e_{33}c_{11}^E + c_{13}^E e_{31})V_S z}{(-c_{11}^E c_{33}^E + (c_{13}^E)^2)h} \tag{29}$$

$$\phi = \frac{V_S z}{h}.$$
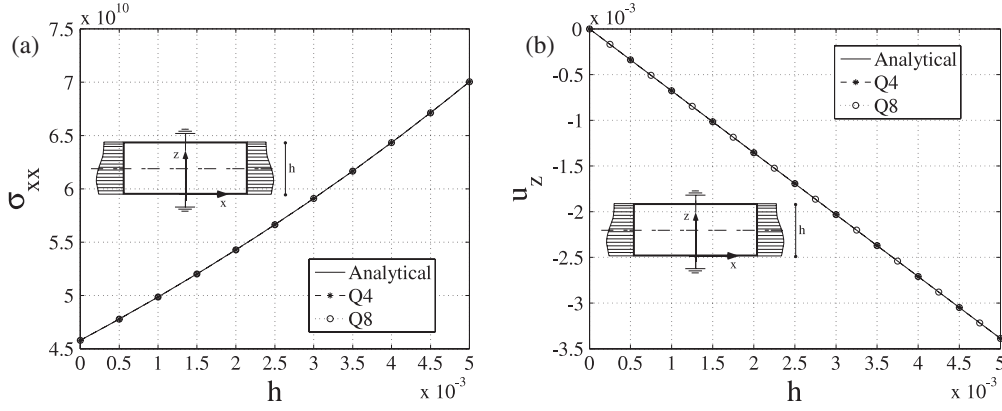
Figure 11. Comparison between numerical and analytical results for a bar *with exponential variation of elastic properties* subjected to normalized uniform strain ($\varepsilon_0 = 1$) in the *x*-direction and short-circuit electrical conditions ($\Delta\phi = 0$). All quantities are evaluated at the nodal locations: (a) stress σ_{xx}; (b) displacement u_z.

Again, the other solutions that consider exponential variation of either elastic, piezoelectric, or dielectric properties are too complex to show, and only the Maple program, written to obtain them, is presented in appendix B.

3. Generalized isoparametric piezoelectric graded finite element

The FGM piezoelectric actuators designed here operate in quasi-static or low-frequency environments where inertia effects can be ignored. The weak formulation of the equilibrium equations of the piezoelectric medium considering linear piezoelectricity is mature and it is given by, for example, (Lerch 1990)

$$\int_\Omega \boldsymbol{\varepsilon}(\mathbf{u})^t \mathbf{c}^E \boldsymbol{\varepsilon}(\mathbf{v}) \, d\Omega + \int_\Omega (\nabla\phi)^t \mathbf{e}^t \boldsymbol{\varepsilon}(\mathbf{v}) \, d\Omega = \int_{\Gamma_\mathbf{t}} \mathbf{t} \cdot \mathbf{v} \, d\Gamma$$

$$\int_\Omega \boldsymbol{\varepsilon}(\mathbf{u})^t \mathbf{e} \nabla\varphi \, d\Omega - \int_\Omega (\nabla\phi)^t \boldsymbol{\epsilon}^S \nabla\varphi \, d\Omega = \int_{\Gamma_d} d\varphi \, d\Gamma \quad (30)$$

for $\mathbf{u}, \phi \in V$ and $\forall \mathbf{v}, \forall \varphi \in V$,

where

$$\mathbf{t} = \boldsymbol{\sigma} \cdot \mathbf{n} \qquad \text{and} \qquad d = \mathbf{D} \cdot \mathbf{n}, \qquad (31)$$

are the mechanical traction and electrical charge, respectively; $\mathbf{n}$ is the normal vector to the surface and

$V = \{\mathbf{v} = v_i \overline{\mathbf{e}}_i, \varphi \text{ with } \mathbf{v} = 0 \text{ on } \Gamma_\mathbf{u}$

and $\varphi = 0 \text{ on } \Gamma_\phi, i = 1 \text{ or } 3\}$,

Ω is the domain of the piezoelectric medium (however, it may also contain non-piezoelectric materials), $\mathbf{v}$ and φ are virtual displacements and virtual electric potential, respectively. The index *i* assumes values 1 or 3 because the problem is considered in the 1–3 plane (or *x*–*z* plane). The piezoceramic is polarized in the local 3 (i.e. *z*) direction (see figure 2).

From the underlying FE formulation, the matrix formulation of the balance equations for the piezoelectric medium is given by (Naillon *et al* 1983)

$$\begin{bmatrix} \mathbf{K}_{uu} & \mathbf{K}_{u\phi} \\ \mathbf{K}_{u\phi}^t & -\mathbf{K}_{\phi\phi} \end{bmatrix} \begin{Bmatrix} \mathbf{U} \\ \boldsymbol{\Phi} \end{Bmatrix} = \begin{Bmatrix} \mathbf{F} \\ \mathbf{Q} \end{Bmatrix} \Longrightarrow [\mathcal{K}]\{\mathcal{U}\} = \{\mathcal{Q}\}, \quad (32)$$

where $\mathbf{K}_{uu}$, $\mathbf{K}_{u\phi}$, and $\mathbf{K}_{\phi\phi}$ denote the stiffness, piezoelectric, and dielectric matrices, respectively, and $\mathbf{F}$, $\mathbf{Q}$, $\mathbf{U}$, and

$\boldsymbol{\Phi}$ are the nodal mechanical force, nodal electrical charge, nodal displacements, and nodal electric potential vectors, respectively. However, in the case of FGM piezoceramics the (macro) properties change continuously inside the piezoceramic domain, which means that they can be described by some continuous function of position $\mathbf{x}$ in the piezoceramic domain, that is

$$\mathbf{c}^E = \mathbf{c}^E(\mathbf{x}); \qquad \mathbf{e} = \mathbf{e}(\mathbf{x}); $$
$$\boldsymbol{\epsilon}^S = \boldsymbol{\epsilon}^S(\mathbf{x}). \qquad (33)$$

From the mathematical definitions of $\mathbf{K}_{uu}$, $\mathbf{K}_{u\phi}$, and $\mathbf{K}_{\phi\phi}$, the material properties must remain inside the matrix integrals and be integrated together by using the graded finite element concept (Kim and Paulino 2002). Properties are continuously interpolated inside each finite element based on property values at each finite element node. It is known that any attempt to approximate the continuous change of material properties by a stepwise function, where a property value is assigned for each finite element, may result in less accurate results with undesirable discontinuities of the stress and strain fields (Kim and Paulino 2002).

In the generalized isoparametric piezoelectric graded finite element, the material properties $\mathbf{c}^E$, $\mathbf{e}$, and $\boldsymbol{\epsilon}^S$ (e.g. at each Gaussian integration point) can be interpolated from the nodal material properties of the element using isoparametric shape functions, which are the same for spatial coordinates (x, y):

$$\mathbf{c}^E = \sum_{i=1}^m N_i \left(\mathbf{c}^E\right)_i; \qquad \mathbf{e} = \sum_{i=1}^m N_i \left(\mathbf{e}\right)_i; $$
$$\boldsymbol{\epsilon}^S = \sum_{i=1}^m N_i \left(\boldsymbol{\epsilon}^S\right)_i, \qquad (34)$$

as illustrated by figure 6, and *m* is the number of element nodes.

Four-node quadrilaterals (Q4) and eight-node quadrilaterals (Q8) for FGM piezoelectrics are implemented in this work using the graded finite element concept. Thus, a fully isoparametric formulation is developed in the sense that the same shape functions are applied to interpolate the unknown displacements and electric potentials, the geometry, and the material properties. Therefore, the actual variation of the material properties may be approximated by the element interpolation functions (e.g. a certain degree of polynomial functions).
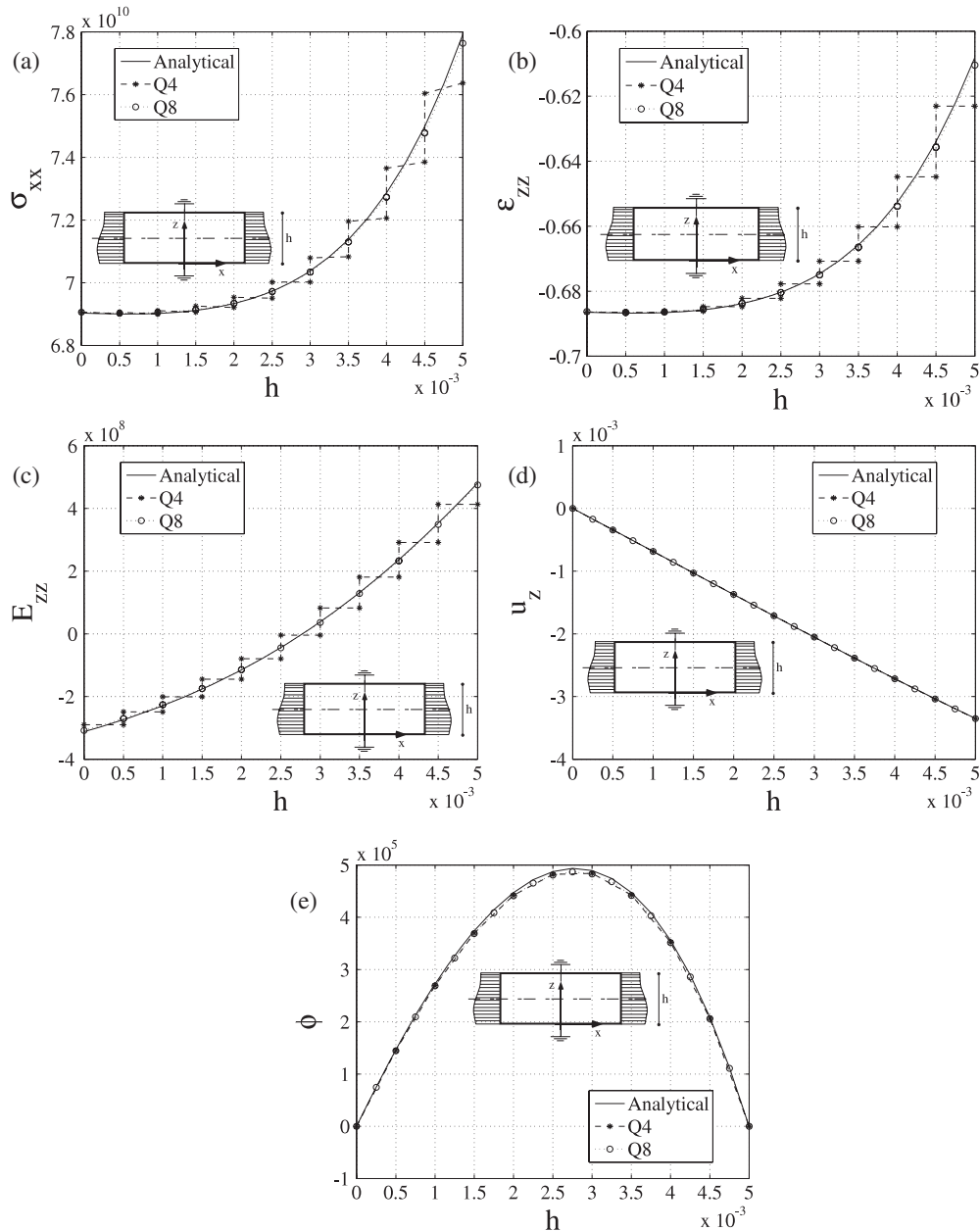
Figure 12. Comparison between numerical and analytical results for a bar *with exponential variation of piezoelectric properties* subjected to normalized uniform strain ($\varepsilon_0 = 1$) in the x-direction and short-circuit electrical conditions ($\Delta\phi = 0$). All quantities are evaluated at the nodal locations: (a) stress σ_{xx}; (b) strain ε_{zz}; (c) electric field E_z; (d) displacement u_z; (e) voltage ϕ.

4. Numerical results

The actual choice of properties and boundary value problems in this section is guided by the analytical solutions derived in section 2. Here, the results from FE simulations are compared with the analytical solutions obtained in section 2. The basic properties described below are adopted, together with the exponential material gradation used in the previous analytical formulation. For the remaining parameters the following values are specified:

$$\varepsilon_0 = 1; \qquad Q = 10^{-6}\ \text{C}; \qquad V_S = 100\ \text{V};$$

$$h = 5 \times 10^{-3}\ \text{m}; \qquad \beta = 85\ \text{m}^{-1}; \qquad \gamma = 322\ \text{m}^{-1};$$

$$c_{11}^{0E} = 7.9 \times 10^{10}\ \text{N m}^{-2}; \qquad c_{13}^{0E} = 5 \times 10^{10}\ \text{N m}^{-2};$$

$$c_{33}^{0E} = 7.3 \times 10^{10}\ \text{N m}^{-2};$$

$$e_{33}^{0} = 3.2\ \text{C m}^{-2}; \qquad e_{31}^{0} = -1.1\ \text{C m}^{-2};$$

$$\alpha = 106\ \text{m}^{-1}; \qquad \epsilon_{33}^{0s}/\epsilon_0 = 1000.$$

The σ_{xx} stress, E_z electric field, normalized u_z displacements, and ϕ electric potential voltage values, are the quantities of interest for comparison purposes. The FE model used in the simulations with corresponding boundary conditions is described in figure 7. The length L is equal to $2h = 10^{-2}$ m. The domain is discretized with 20×10 elements

2417
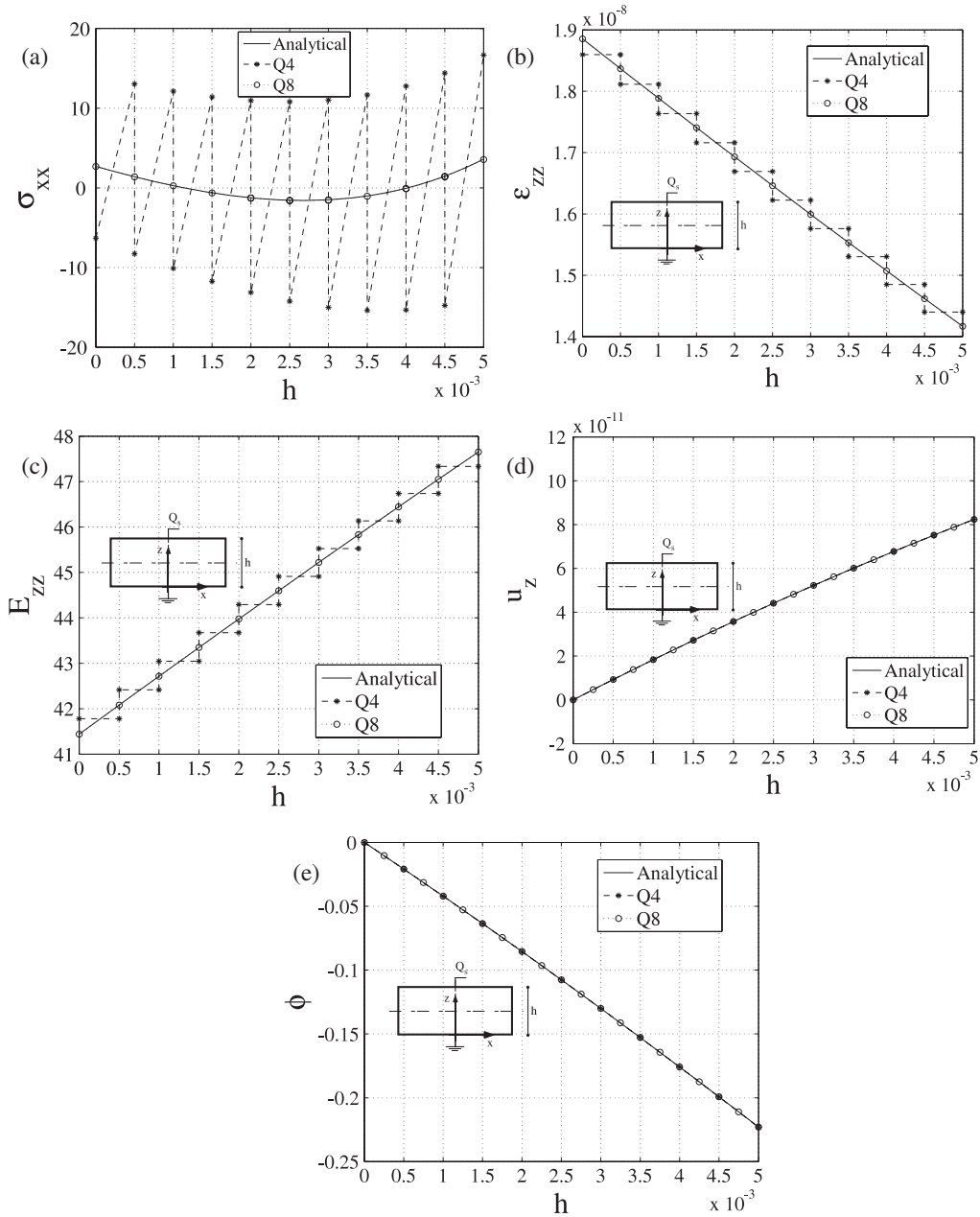
Figure 13. Comparison between numerical and analytical results for a bar *with exponential variation of elastic properties* subjected to electrical charge excitation per area (Q_s) and no mechanical load. All quantities are evaluated at the nodal locations: (a) stress σ_{xx}; (b) strain ε_{zz}; (c) electric field E_z; (d) displacement u_z; (e) voltage ϕ.

under the plane strain assumption. For all examples, 2×2 Gauss quadrature is employed. All the numerical stress values reported here are nodal values extrapolated directly from the Gauss points and without any averaging. A simple FE code was implemented in MATLAB to obtain the results presented in this section.

4.1. Uniform strain and open-circuit electrical conditions

In the first case, the bar is subjected to normalized uniform strain ($\varepsilon_0 = 1$) due to a displacement equal to L (thus, unit strain) in the x-direction, and open-circuit electrical conditions ($Q = 0$). For an exponential variation of elastic properties,

figures 8(a)–(e) show both analytical and numerical solutions (Q4 and Q8 elements) for σ_{xx}, ϵ_{zz}, E_z, u_z, and ϕ, evaluated at the nodal points, respectively, versus z. Figures 9 and 10(a)–(e) present analogous comparison for an exponential variation of piezoelectric and dielectric properties, respectively. According to equations (5) and (7), the stress σ_{xx} is uniform in the x-direction and thus, graphs of figures 8–10 are valid for the entire range of x coordinates ($0 \leqslant x \leqslant L$). The deformed shapes for these three cases are similar, however, when material gradation is considered either with electrical potential or charge excitation, then bending occurs, as described below.

We notice that the material gradation affects the σ_{xx}, ε_{zz}, and E_z distributions, which assume constant values in the
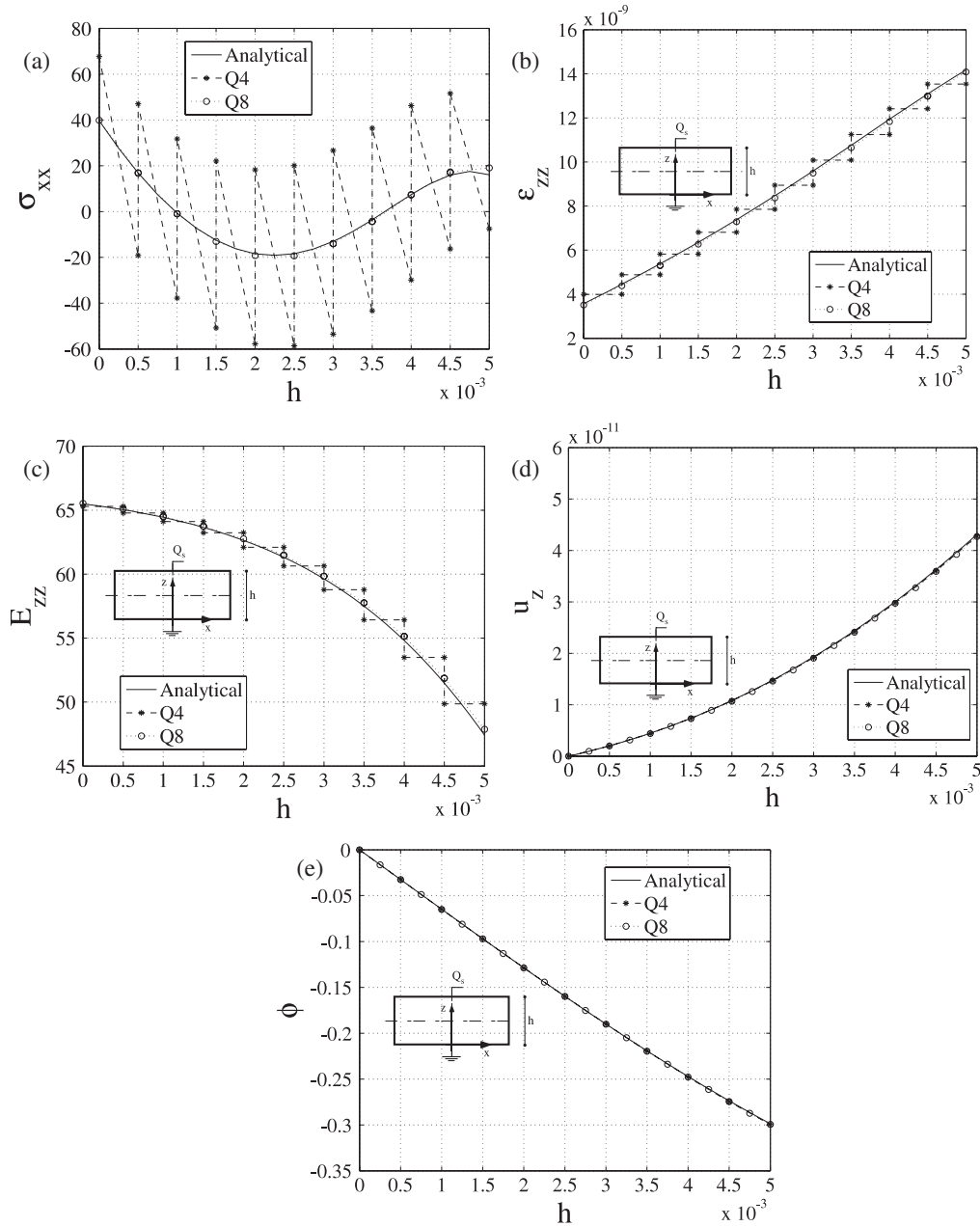
Figure 14. Comparison between numerical and analytical results for a bar *with exponential variation of piezoelectric properties* subjected to electrical charge excitation per area (Q_s) and no mechanical load. All quantities are evaluated at the nodal locations: (a) stress σ_{xx}; (b) strain ε_{zz}; (c) electric field E_z; (d) displacement u_z; (e) voltage ϕ.

homogeneous case (see equation (14)). The exponential elastic and piezoelectric property gradations cause the stress σ_{xx} to increase, while the dielectric property gradation causes the stress σ_{xx} to decrease with z-direction. The ε_{zz} distribution increases with z-direction for piezoelectric property gradation and decreases with z-direction for elastic and dielectric property gradations. The E_z distribution increases with z-direction for elastic and piezoelectric property gradations, and decreases for dielectric property gradation. A highly nonlinear distribution of σ_{xx}, ε_{zz}, and E_z is observed for the piezoelectric property gradation. This nonlinearity seems to be less pronounced for elastic and dielectric property gradations. Thus, we conclude that piezoelectric property gradation seems

to have a stronger influence than elastic and dielectric property gradations in this problem.

The Q4 elements are able to represent the σ_{xx} distribution for elastic property gradation, however, a strong inter-element discontinuity appears for piezoelectric and dielectric property gradations. No discontinuity is observed for u_z and ϕ distributions for all property gradations, and their values are quite close to the corresponding analytical values. However, a discontinuity is observed for ε_{zz} and E_z distributions in all cases when using Q4 elements. The Q8 elements are able to represent σ_{xx}, ε_{zz}, and E_z distributions for all cases without discontinuity. All Q8 numerical results are quite close to the corresponding analytical values.
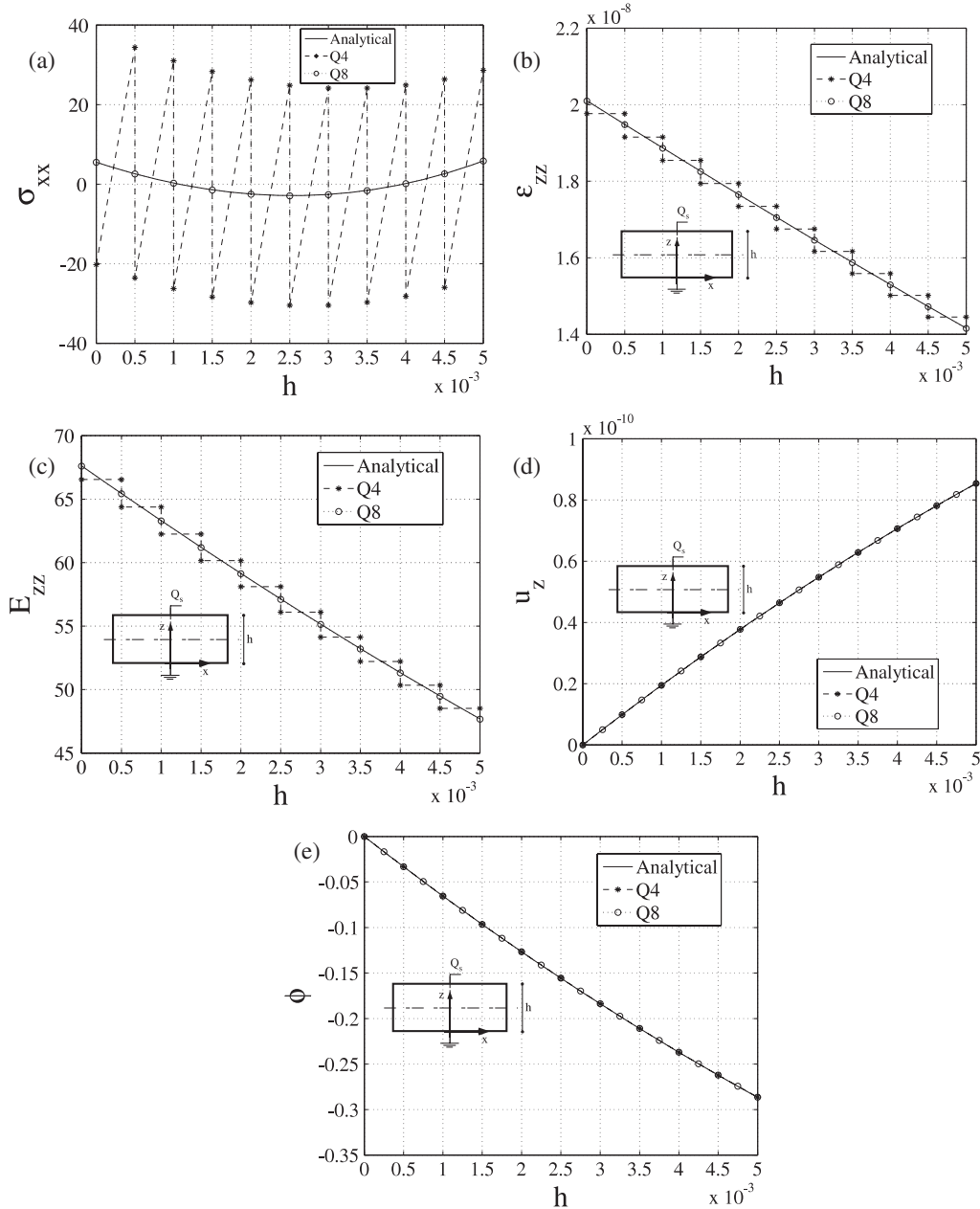
Figure 15. Comparison between numerical and analytical results for a bar *with exponential variation of dielectric properties* subjected to electrical charge excitation per area (Q_s) and no mechanical load. All quantities are evaluated at the nodal locations: (a) stress σ_{xx}; (b) strain ε_{zz}; (c) electric field E_z; (d) displacement u_z; (e) voltage ϕ.

4.2. Uniform strain and short-circuit electrical conditions

In the second case, the bar is subjected to normalized uniform strain ($\varepsilon_0 = 1$) due to a displacement equal to L (thus, unit strain) in the x-direction and short-circuit electrical conditions ($\Delta\phi = 0$). Figures 11(a) and (b) show analytical and numerical (Q4 and Q8 elements) solutions for σ_{xx} and u_z, evaluated at the nodal locations, respectively, versus z, considering an exponential variation of elastic properties. The electric potential ϕ and the electric field E_z are not plotted because constant values equal to zero inside the piezoceramic are obtained as a result for this case. The strain ε_{zz} is also not plotted because a constant value equal to the homogeneous case is obtained, as expected

from equation (21). Figures 12(a)–(e) present analogous comparison for an exponential variation of piezoelectric properties, however, including the plots of ε_{zz}, ϕ, and E_z (in addition to σ_{zz} and u_z). The graphs for an exponential variation of dielectric properties are not shown because, as mentioned in section 2, they do not influence the solutions of σ_{xx}, u_z, ϕ, and E_z for this load case, which have the same solutions as in the homogeneous case (no material variation). The deformed shapes for these three cases are similar.

The elastic property gradation affects mainly the σ_{xx} distribution, while the piezoelectric property gradation affects all quantities. A highly nonlinear distribution of σ_{xx}, ε_{zz}, E_z, and ϕ is observed for the piezoelectric property gradation. This nonlinearity is less pronounced for the elastic property
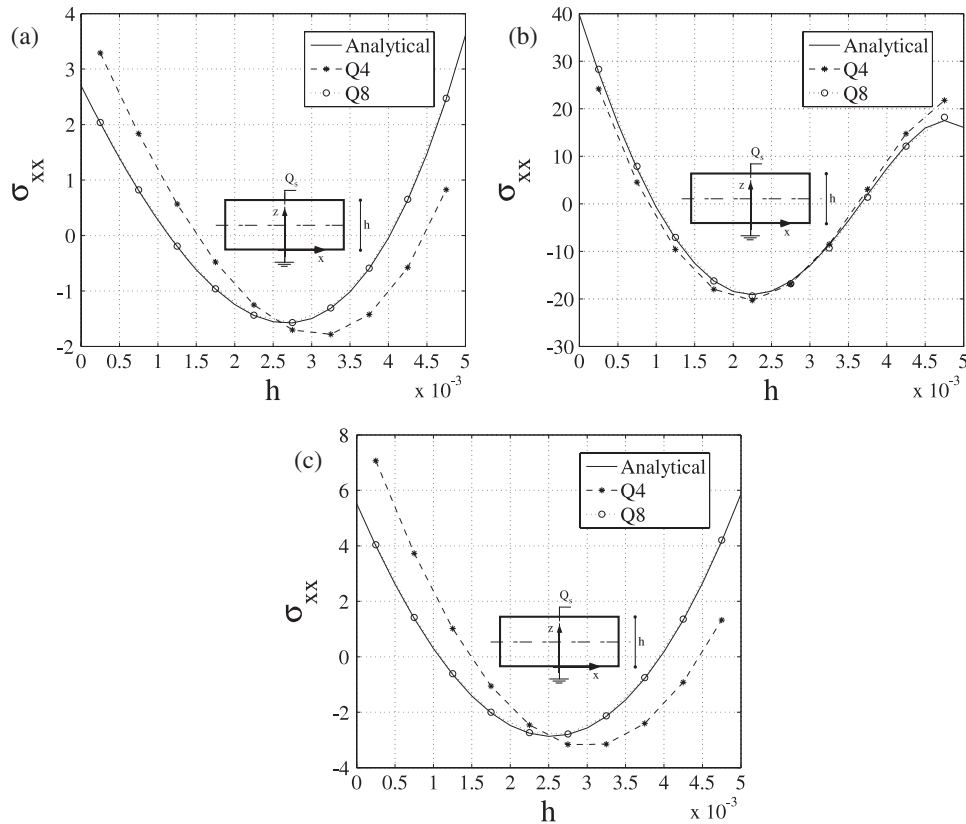
Figure 16. Comparison between numerical and analytical results of stress values (σ_{xx}) evaluated at the element centroid for a bar subjected to electrical charge excitation per area (Q_s) and no mechanical load: (a) *exponential variation of elastic properties*; (b) *exponential variation of piezoelectric properties*; (c) *exponential variation of dielectric properties*.

gradation. The stress σ_{xx} value increases with z-direction for both property gradations (i.e. elastic and piezoelectric), as in the previous example. The electric field E_z increases with z-direction for the piezoelectric property gradation. As shown in figure 12(e), the ϕ distribution has a parabolic shape, indicating high voltages inside the piezoceramic even though short-circuit electrical conditions are imposed. This situation is quite different from homogeneous and elastic property gradation cases, in which the electric potential is null inside the piezoceramic. Again, we conclude that piezoelectric property gradation has a stronger influence than the elastic and dielectric property gradations.

The Q4 elements are able to represent the σ_{xx}, ε_{zz}, and E_z distributions for elastic property gradation, however, a strong inter-element discontinuity appears for the piezoelectric property gradation. No discontinuity is observed for u_z and ϕ distributions for all property gradations and their values are quite close to the corresponding analytical values. The Q8 elements are able to represent the σ_{xx}, ε_{zz}, and E_z distributions for all cases without discontinuity, as in the previous example. Again, all Q8 numerical results are quite close to the corresponding analytical values.

4.3. Electrical charge excitation

In the third case, the bar is subjected to electrical charge excitation per area (Q_s) and no mechanical load. Analytical and numerical solutions for σ_{xx}, ε_{zz}, E_z, u_z, and ϕ, evaluated at nodal locations, versus the z-coordinate, are shown in figures 13(a)–(e), respectively, considering an exponential variation of elastic properties. Additional comparisons are presented in figures 14 and 15(a)–(d) for an exponential variation of piezoelectric and dielectric properties, respectively.

The comparative σ_{xx} stress distribution indicates that there is bending of the FGM piezoceramic, especially for the piezoelectric property gradation case. In this instance, the bending deformation configuration is different from those for the elastic and dielectric property gradation cases. Compare figure 14(a) with 13(a) and 15(a), respectively. A nonlinear distribution of σ_{xx} and a slightly nonlinear distribution for u_z with z-direction is observed for all property gradations. A nonlinear distribution of E_z with z-direction is observed for the piezoelectric property gradation case. The variation of other quantities is almost linear with the z-direction. The strain ε_{zz} value increases with z-direction for the piezoelectric property gradation case and decreases for the elastic and dielectric property gradation cases. Moreover, the electric field E_z increases with z-direction for elastic property gradation and decreases for piezoelectric and dielectric property gradations.

The σ_{xx} numerical results calculated using the Q4 element show strong inter-element discontinuity for all property gradations. The stress distribution evaluated at the element centroid also does not match the analytical value for all
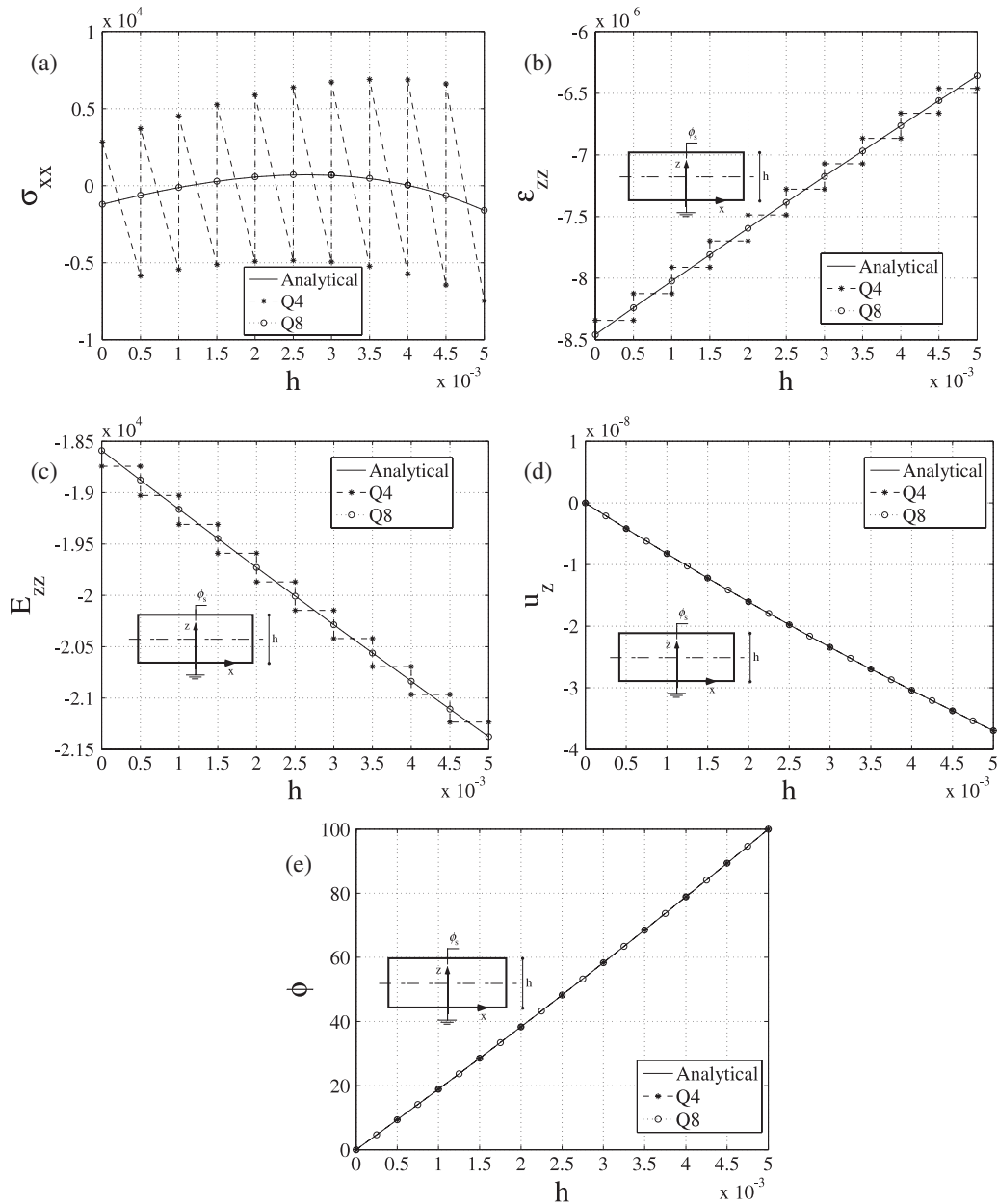
Figure 17. Comparison between numerical and analytical results for a bar *with exponential variation of elastic properties* subjected to electrical voltage excitation (V_s) and no mechanical load. All quantities are evaluated at the nodal locations: (a) stress σ_{xx}; (b) strain ε_{zz}; (c) electric field E_z; (d) displacement u_z; (e) voltage ϕ.

property gradations as shown in figures 16(a)–(c). This stress distribution discontinuity seems to be compatible with what is reported by Kim and Paulino (2002) when modeling non-piezoelectric FGMs subjected to a load parallel to the property gradation direction. By applying an electrical charge excitation, a similar situation seems to occur. A discontinuity also occurs for the distribution of ε_{zz} and E_z calculated using Q4 elements. No discontinuity is observed for the distribution of u_z and ϕ for all property gradations and their values are quite close to the corresponding analytical values. However, Q8 elements are able to represent the distribution of σ_{xx}, ε_{zz}, and E_z for all cases without discontinuity and matching analytical results, as in the previous examples.

4.4. Electrical voltage excitation

Finally, in the fourth case investigated, the bar is subjected to electrical voltage excitation (V_s) and no mechanical load. Analytical and numerical solutions for σ_{xx}, ε_{zz}, E_z, u_z, and ϕ, evaluated at nodal locations, versus the z-coordinate, are shown in figures 17(a)–(e), respectively, considering an exponential variation of elastic properties. Additional comparisons are presented in figures 18 and 19(a)–(e) for an exponential variation of piezoelectric and dielectric properties, respectively.

Similarly to the previous example, by analysing the σ_{xx} stress distribution for all cases, we can notice that bending occurs due to the property gradation. Again, the
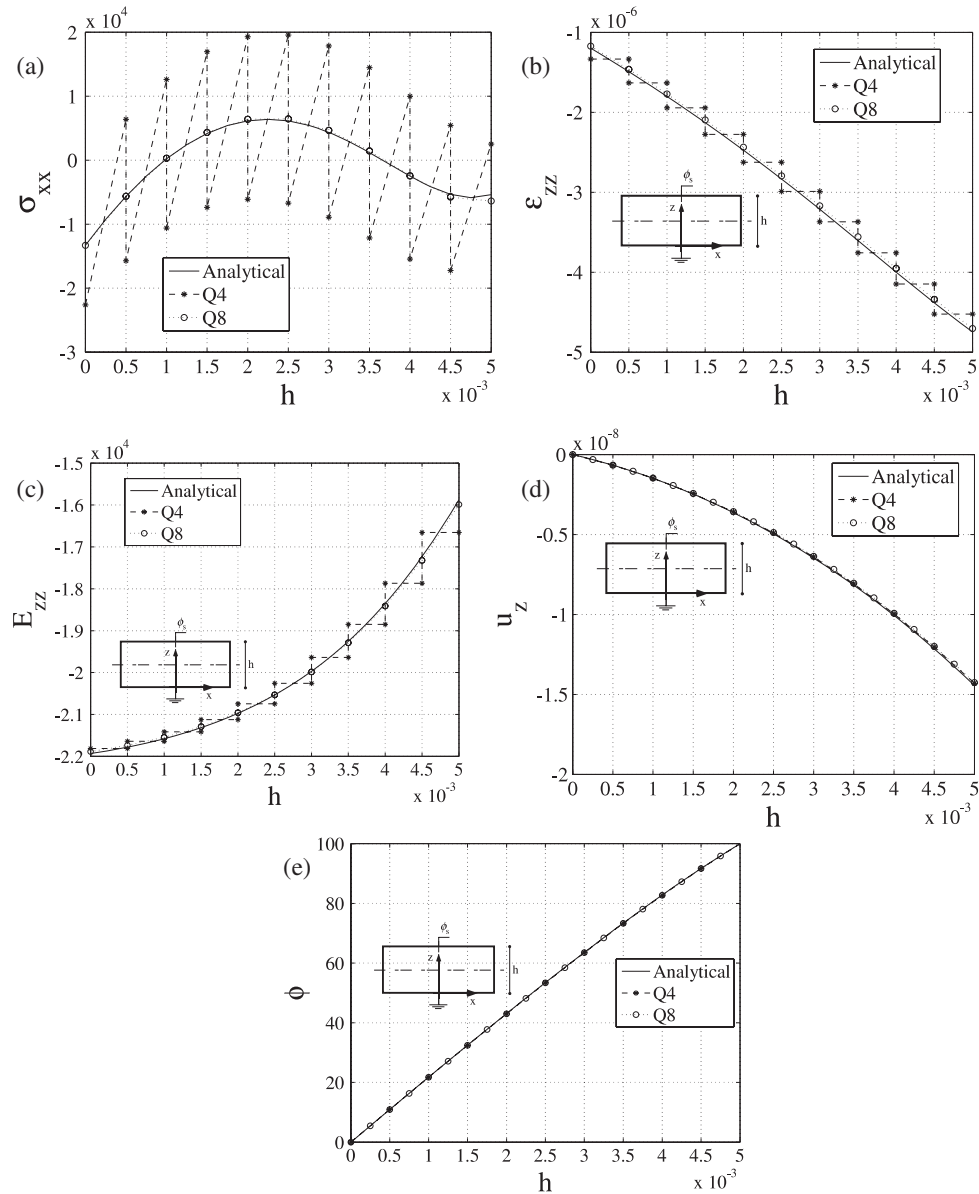
Figure 18. Comparison between numerical and analytical results for a bar *with exponential variation of piezoelectric properties* subjected to electrical voltage excitation (V_s) and no mechanical load. All quantities are evaluated at the nodal locations: (a) stress σ_{xx}; (b) strain ε_{zz}; (c) displacement u_z; (d) voltage ϕ.

bending occurs differently for piezoelectric property gradation in relation to elastic and dielectric property gradations. A nonlinear distribution of σ_{xx} with z-direction is observed for all property gradations. A nonlinear distribution of u_z and E_z occurs for the piezoelectric property gradation. The variation of other quantities is almost linear with z-direction. The strain ε_{zz} value decreases with z-direction for piezoelectric property gradation, and increases for elastic and dielectric property gradations. The electric field E_z increases with z-direction for piezoelectric and dielectric property gradations, and decreases for elastic property gradation.

Again, a strong discontinuity of the σ_{xx} numerical results calculated using the Q4 element can be observed for all property gradations. The stress distribution evaluated at the element centroid also does not match the analytical results

for all property gradations, as shown in figures 20(a)–(c). This behavior is compatible with the behavior observed in the previous example. Inter-element discontinuities for ε_{zz} and E_z also occurs using Q4 elements. No discontinuity is observed for the distributions of u_z and ϕ for all property gradations, and their values are quite close to the corresponding analytical results. The Q8 elements are able to represent σ_{xx}, ε_{zz}, and E_z distributions for all cases without discontinuity and matching analytical results, as in the previous examples.

5. Conclusions

A finite element method for nonhomogeneous piezoelectric materials using a generalized isoparametric formulation based on the graded finite element concept has been investigated.
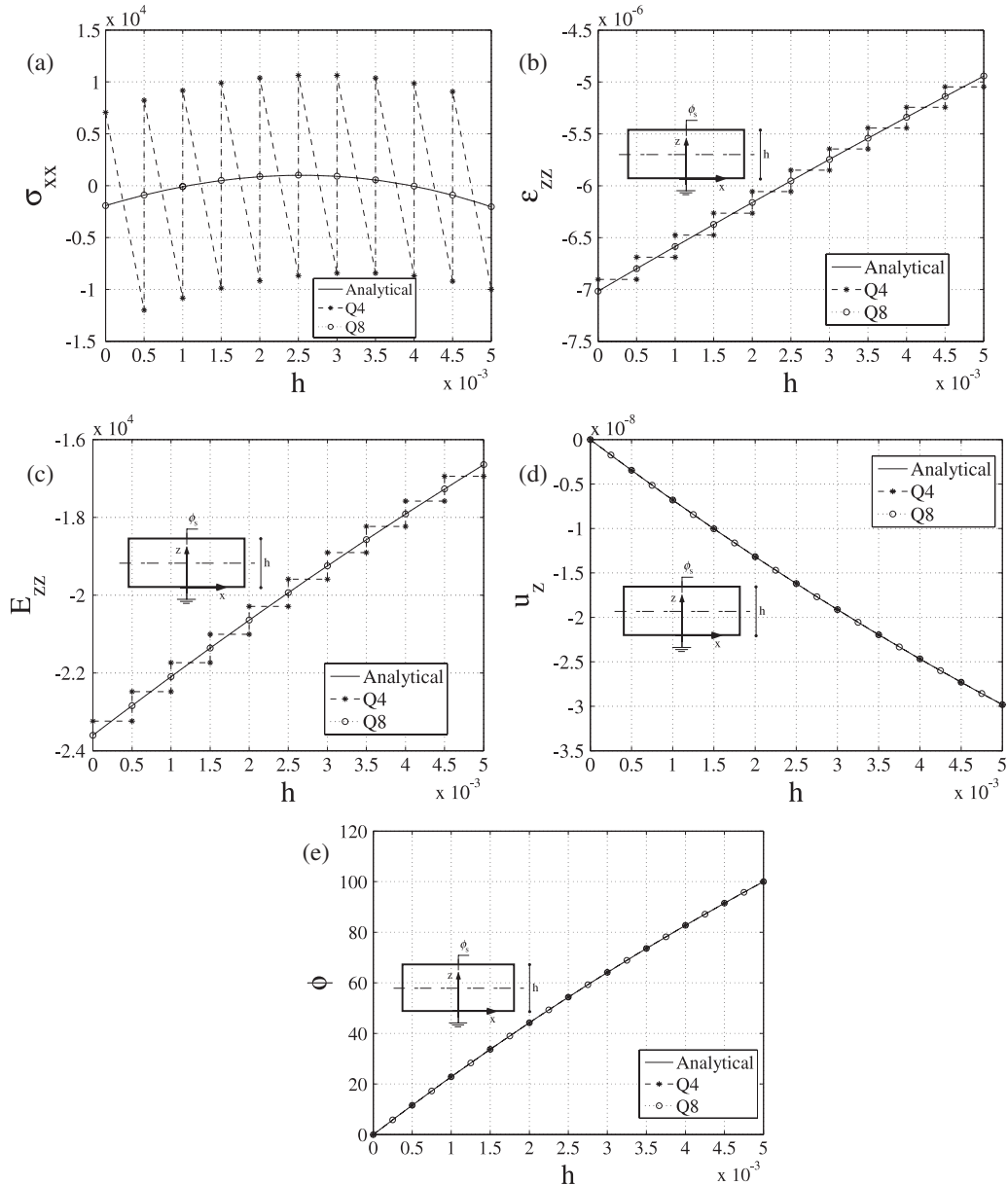
Figure 19. Comparison between numerical and analytical results for a bar *with exponential variation of dielectric properties* subjected to electrical voltage excitation (V_s) and no mechanical load. All quantities are evaluated at the nodal locations: (a) stress σ_{xx}; (b) strain (ε_{zz}); (c) electric field E_z; (d) displacement u_z; (e) voltage ϕ.

Through this approach the properties change smoothly inside the element providing a continuum material distribution, which is appropriate to model FGMs. Four-node quadrilaterals (Q4) and eight-node quadrilaterals (Q8) for piezoelectric FGMs have been implemented.

An analytical model has been derived based on mechanical and piezoelectric constitutive equations in order to verify the accuracy of finite element simulations and to understand the influence of material property gradation in the behavior of the piezoelectric FGM. As an overall observation, the exponential gradation of elastic, piezoelectric, and dielectric properties causes change in stress and electric potential distribution inside the piezoceramic domain, which in turn, can influence the FGM piezoactuator performance.

The behavior of graded piezoelectric elements under various loading conditions with respect to the analytical solutions has been discussed and compared. The examples consider two-dimensional models with the plane strain assumption. To address the influence of material property variation, the elastic, piezoelectric, and dielectric properties have been graded separately, considering exponential variation; and quantities such as displacement, electric potential, stress, electric field, and electric displacement have been obtained. Several domains with continuously nonhomogeneous materials are considered under fixed grip (open and short-circuit conditions), electrical charge excitation, and electrical voltage excitation.

The stress (σ_{xx}) and strain (ε_{zz}) results show that the graded Q4 element is not able to represent the fields properly,
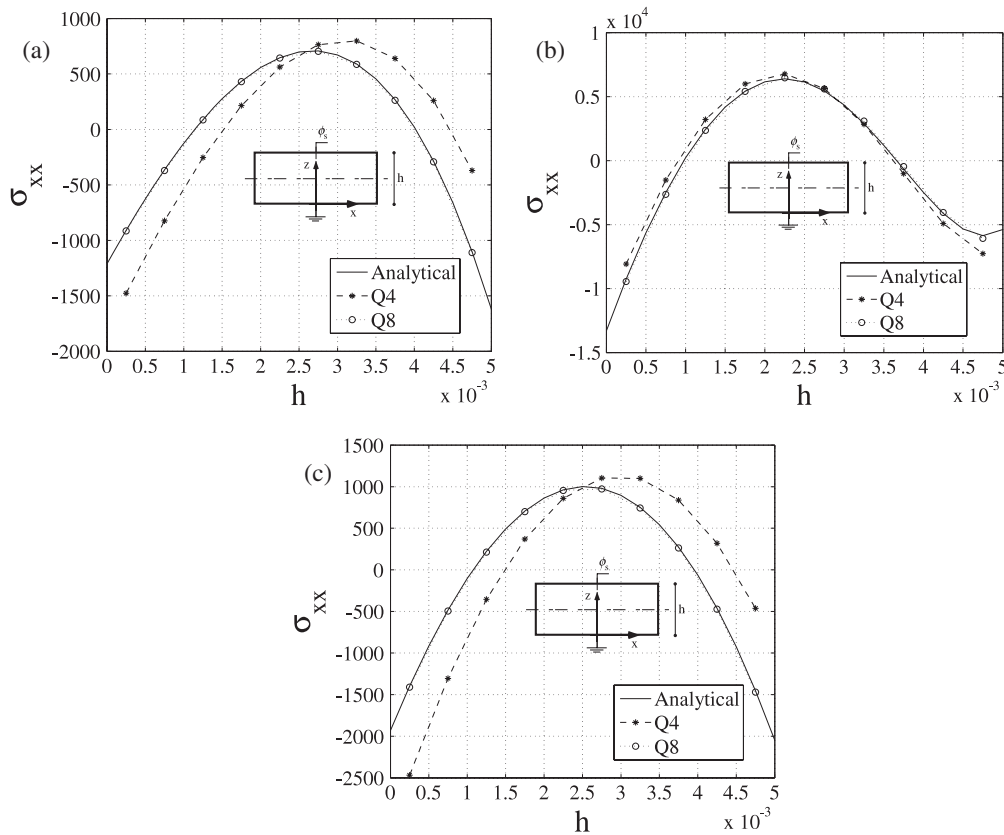
Figure 20. Comparison between numerical and analytical results of stress values (σ_{xx}) evaluated at the element centroid for a bar subjected to electrical voltage excitation (V_s) and no mechanical load: (a) *exponential variation of elastic properties*; (b) *exponential variation of piezoelectric properties*; (c) *exponential variation of dielectric properties*.

giving strong discontinuities for some load cases, even though displacement (u_z) and electric potential (ϕ) are obtained with reasonable accuracy. However, the Q8 element is able to model the FGM piezoceramic behavior accurately, giving smooth and accurate stress, strain, and electric field profiles. One should be careful when using graded elements with linear shape functions, such as Q4, as they may lose accuracy for calculation of stress, strain, and electric field, mainly when the electrical or mechanical loads are parallel to the material gradient direction. A similar conclusion was reached by Kim and Paulino (2002) for non-piezoelectric FGM materials.

Acknowledgments

Appendix A. Nomenclature

List of Symbols:

$(.)_x$, $(.)_y$, $(.)_z$	x-component, y-component, z-component
(x, z)	coordinate system
A, B, C	variables
A_S	surface electrode area
$\mathbf{c}^E$	elastic tensor
c_{ij}^E	coefficient of elastic tensor $\mathbf{c}^E$
c_{ij}^{0E}	coefficient of elastic tensor $\mathbf{c}^E$ of basic material
d	distributed electrical charge
D_i	electric displacement component
$\mathbf{D}$	electrical displacement vector
$\mathbf{e}$	piezoelectric tensor
e_{ij}	coefficient of piezoelectric tensor $\mathbf{e}$
e_{ij}^0	coefficient of piezoelectric tensor $\mathbf{e}$ of basic material
$e^{(\cdot)}$	exponential function
$\overline{\mathbf{e}}_i$	unit vector
$\mathbf{E}$	electrical field
E_i	electric field component
$f(\cdot)$	function
$\mathbf{F}$	nodal mechanical force
h	thickness
$\mathbf{n}$	normal vector

Q	electrical charge
Q_s	applied electrical charge
Q	nodal electrical charge
$\{\mathcal{Q}\}$	force and electrical charge vector
$\mathbf{K}_{uu}$	stiffness matrix
$\mathbf{K}_{u\phi}$	piezoelectric matrix
$\mathbf{K}_{\phi\phi}$	dielectric matrix
$[\mathcal{K}]$	system matrix
L	length
$\log(\cdot)$	log function
$\tan^{-1}(\cdot)$	inverse tangent function
m	number of element nodes
$N_I(\mathbf{x})$	finite element shape function
t	traction
u	displacement field
u_i and v_i	node i horizontal and vertical displacement, respectively,
U	nodal displacements
$\{\mathcal{U}\}$	displacement and electrical degrees of freedom vector
v	virtual displacement
V	space
V_s	applied electrical voltage
x	position coordinate vector
Δ	difference operator
α	coefficient of exponential material variation of elastic property
β	coefficient of exponential material variation of piezoelectric property
γ	coefficient of exponential material variation of dielectric property
ϵ_{ij}^S	coefficient of dielectric tensor $\boldsymbol{\epsilon}^S$
ϵ_{ij}^{0S}	coefficient of dielectric tensor $\boldsymbol{\epsilon}^S$ of basic material
$\boldsymbol{\epsilon}^S$	dielectric tensor
ε_{ij}	strain component
$\boldsymbol{\varepsilon}(\mathbf{u})$	strain
ε_0	applied uniform strain
ϕ	electric potential
$\boldsymbol{\Phi}$	nodal electric potential vector
$\Gamma_{\mathbf{t}}$	surface of applied mechanical traction
Γ_d	surface of applied electrical voltage
$\Gamma_{\mathbf{u}}$	surface of prescribed displacements
Γ_ϕ	surface of prescribed electrical degrees of freedom
φ	virtual electric potential
σ_{ij}	stress component
∇_{sym}	symmetric part of gradient operator
$\boldsymbol{\sigma}$	stress tensor
Ω	domain
$\nabla\phi$	gradient of electrical potential
∇	gradient operator

Appendix B. Maple Programs

The following codes were run with Maple 7.0. Only a few basic Maple operations such as linear system solution, integration and substitution, are employed, and thus it is likely that, with relatively minor changes, these scripts would work with

other symbolic computation systems. The naming of variables follows the notation in the paper fairly closely, and we hope that the codes are self-explanatory.

B.1. Bar subjected to uniform strain (ε_0) in the x-direction and open-circuit electrical conditions ($Q = 0$)

B.1.1. Exponential elastic property gradation.
```
restart;
with(linalg);
c13:=c013*exp(beta*z);
c33:=c033*exp(beta*z)
c11:=c011*exp(beta*z);
AA:=array([[-1,c13,e31],[0,c33,e33],
  [0,e33,-eps33]]);
FF:=array([-c11*eps0,
  -c13*eps0,-e31*eps0]);
UU:=linsolve(AA,FF);
sigmaxx:=simplify(UU[1]);
epszz:=simplify(UU[2]);
Ez:=-simplify(UU[3]);
uz:=simplify(int(epszz,0..z));
phi:=simplify(int(-Ez,0..z));
```

B.1.2. Exponential piezoelectric property gradation.
Substitute the third, fourth, and fifth lines of the program above by
```
e31:=e031*exp(g*z);
e33:=e033*exp(g*z);
```

B.1.3. Exponential dielectric property gradation.
Substitute the third, fourth, and fifth lines of the program above by
```
eps33:=eps033*exp(alpha*z);
```

B.2. Bar subjected to uniform strain (ε_0) in the x-direction and short-circuit electrical conditions ($\Delta\phi = 0$)

B.2.1. Exponential elastic property gradation.
```
restart;
with(linalg);
c13:=c013*exp(beta*z);
c33:=c033*exp(beta*z);
c11:=c011*exp(beta*z);
AA:=array([[-1,c13,e31],[0,c33,e33],
  [0,e33,-eps33]]);
FF:=array([-c11*eps0,-c13*eps0,
  -e31*eps0+C]);
UU:=linsolve(AA,FF);
Ez:=-UU[3];
eq1:=simplify(int(Ez,z=0..h));
sol:=solve({eq1=0},{C});
sigmaxx:=UU[1];
epszz:=simplify(UU[2]);
epszzn:=simplify(subs(sol,epszz));
Ezn:=simplify(subs(sol,Ez));
sigmaxxn:=simplify(subs(sol,sigmaxx));
uz:=simplify(int(epszzn,0..z));
phi:=simplify(int(-Ezn,0..z));
```

B.2.2. Exponential piezoelectric property gradation. Substitute the third, fourth, and fifth lines of the program above by

```
e31:=e031*exp(g*z);
e33:=e033*exp(g*z);
```

B.2.3. Exponential dielectric property gradation. Substitute the third, fourth, and fifth lines of the program above by

```
eps33:=eps033*exp(alpha*z);
```

B.3. Bar subjected to electrical charge excitation per area (Q_s) and no mechanical load

B.3.1. Exponential elastic property gradation.
```
restart;
with(linalg);
c13:=c013*exp(beta*z);
c33:=c033*exp(beta*z);
c11:=c011*exp(beta*z);
AA:=array([[-1,c13,e31],[0,c33,e33],
  [0,e33,-eps33]]);
FF:=array([-c11*(A*z+B),-c13*(A*z+B),
  -e31*(A*z+B)+QS]);
UU:=linsolve(AA,FF);
sigmaxx:=UU[1];
epszz:=UU[2];
Ez:=-UU[3];
eq1:=int(sigmaxx,z=0..h);
eq2:=int(sigmaxx*z,z=0..h);
sol:=solve({eq1=0,eq2=0},{A,B});
epszzn:=simplify(subs(sol,epszz));
Ezn:=simplify(subs(sol,Ez));
sigmaxxn:=simplify(subs(sol,sigmaxx));
uz:=simplify(int(epszzn,z=0..z));
phi:=simplify(int(-Ezn,z=0..z));
```

B.3.2. Exponential piezoelectric property gradation. Substitute the third, fourth, and fifth lines of the program above by

```
e31:=e031*exp(g*z);
e33:=e033*exp(g*z);
```

B.3.3. Exponential dielectric property gradation. Substitute the third, fourth, and fifth lines of the program above by

```
eps33:=eps033*exp(alpha*z);
```

B.4. Bar subjected to electrical voltage excitation (V_s) and no mechanical load

B.4.1. Exponential elastic property gradation.
```
restart;
with(linalg);
c13:=c013*exp(beta*z);
c33:=c033*exp(beta*z);
c11:=c011*exp(beta*z);
AA:=array([[-1,c13,e31],[0,c33,e33],
  [0,e33,-eps33]]);
FF:=array([-c11*(A*z+B),-c13*(A*z+B),
  -e31*(A*z+B)+C]);
```

```
UU:=linsolve(AA,FF);
sigmaxx:=UU[1];
epszz:=UU[2];
Ez:=-UU[3];
eq1:=int(sigmaxx,z=0..h);
eq2:=int(sigmaxx*z,z=0..h);
eq3:=int(-Ez,z=0..h);
sol:=solve({eq1=0,eq2=0,eq3=VS},{A,B,C});
epszzn:=simplify(subs(sol,epszz));
sigmaxxn:=simplify(subs(sol,sigmaxx));
Ezn:=simplify(subs(sol,Ez));
uz:=simplify(int(epszzn,z=0..z));
phi:=simplify(int(-Ezn,z=0..z));
```

B.4.2. Exponential piezoelectric property gradation. Substitute the third, fourth, and fifth lines of the program above by

```
e31:=e031*exp(g*z);
e33:=e033*exp(g*z);
```

B.4.3. Exponential dielectric property gradation. Substitute the third, fourth, and fifth lines of the program above by

```
eps33:=eps033*exp(alpha*z);
```

References

Almajid A, Taya M and Hudnut S 2001 Analysis of out-of-plane displacement and stress field in a piezocomposite plate with functionally graded microstructure *Int. J. Solids Struct.* **38** 3377–91

Ballato J, Schwartz R and Ballato A 2001 Network formalism for modeling functionally graded piezoelectric plates and stacks *IEEE Trans. Ultrason. Ferroelectr. Freq. Control* **48** 462–76

Banks-Sills L, Eliasi R and Berlin Y 2002 Modeling of functionally graded materials in dynamic analyses *Composites* B **33** 7–15

Chakraborty A and Gopalakrishnan S 2003 A spectrally formulated finite element for wave propagation analysis in functionally graded beams *Int. J. Solids Struct.* **40** 2421–48

Chen Y H, Li T and Ma J 2003 Investigation on the electrophoretic deposition of a fgm piezoelectric monomorph actuator *J. Mater. Sci.* **38** 2803–7

Elka E, Elata D and Abramovich H 2004 The electromechanical response of multilayered piezoelectric structures *J. Microelectromech. Syst.* **13** 332–41

Huang D J, Ding H J and Chen W Q 2007 Piezoelasticity solutions for functionally graded piezoelectric beams *Smart Mater. Struct.* **16** 687–95

Ikeda T 1996 *Fundamentals of Piezoelectricity* (Oxford: Oxford University Press)

Kim J H and Paulino G H 2002 Isoparametric graded finite elements for nonhomogeneous isotropic and orthotropic materials *ASME J. Appl. Mech.* **69** 502–14

Lerch R 1990 Simulation of piezoelectric devices by two- and three-dimensional finite elements *IEEE Trans. Ultrason. Ferroelectr. Freq. Control* **37** 233–47

Miyamoto Y, Kaysser W A, Rabin B H, Kawasaki A and Ford R G 1999 *Functionally Graded Materials: Design, Processing and Applications* (Dordrecht: Kluwer–Academic)

Naillon M, Coursant R H and Besnier F 1983 Analysis of piezoelectric structures by a finite element method *Acta Eletron.* **25** 341–62

Qiu J, Tani J, Ueno T, Morita T, Takahashi H and Du H 2003 Fabrication and high durability of functionally graded piezoelectric bending actuators *Smart Mater. Struct.* **12** 115–21

Santare M H and Lambros J 2000 Use of graded finite elements to model the behavior of nonhomogeneous materials *Trans. ASME J. Appl. Mech.* **67** 819–22

Santare M H, Thamburaj P and Gazonas G A 2003 The use of graded finite elements in the study of elastic wave propagation in continuously nonhomogeneous materials *Int. J. Solids Struct.* **40** 5621–34

Shi Z F and Chen Y 2004 Functionally graded piezoelectric cantilever beam under load *Arch. Appl. Mech.* **74** 237–47

Suresh S and Mortensen A 1988 *Fundamentals of Functionally Graded Materials* (London: IOM Communications)

Taya M, Almajid A A, Dunn M and Takahashi H 2003 Design of bimorph piezo-composite actuators with functionally graded microstructure *Sensors Actuators* A **107** 248–60

Thamburaj P, Santare M H and Gazonas G A 2003 The effect of graded strength on damage propagation in continuously nonhomogeneous materials *Trans. ASME J. Eng. Mater. Technol.* **125** 412–17

Yang J and Xiang H J 2007 Thermo-electro-mechanical characteristics of functionally graded piezoelectric actuators *Smart Mater. Struct.* **16** 784–97

Ying C and Zhifei S 2005 Exact solutions of functionally gradient piezothermoelastic cantilevers and parameter identification *J. Intell. Mater. Syst. Struct.* **16** 531–9

Zhang Z and Paulino G H 2007 Wave propagation and dynamic analysis of smoothly graded heterogeneous continua using graded finite elements *Int. J. Solids Struct.* **44** 3601–26

Zhifei S 2002 General solution of a density functionally gradient piezoelectric cantilever and its applications *Smart Mater. Struct.* **11** 122–9

Zhu X H and Meng Z Y 1995 Operational principle, fabrication and displacement characteristics of a functionally gradient piezoelectric ceramic actuator *Sensors Actuators* A **48** 169–76